Green fluorescent protein-like pigments optimize the internal light environment in symbiotic reef building corals

Elena Bollati[1,2,3*], Niclas H. Lyndby[2,4], Cecilia D'Angelo[1], Michael Kühl[2,5], Jörg Wiedenmann[1] & Daniel Wangpraseurt[6,7,8*]

[1]Coral Reef Laboratory, School of Ocean and Earth Science, University of Southampton, United Kingdom

[2]Marine Biology Section, Department of Biology, University of Copenhagen, Strandpromenaden 5, DK-3000 Helsingør, Denmark

[3]Department of Biological Sciences, National University of Singapore, 16 Science Drive 4, Singapore 117558

[4]Laboratory for Biological Geochemistry, School of Architecture, Civil and Environmental Engineering, Ecole Polytechnique Fédérale de Lausanne (EPFL), CH-1015 Lausanne, Switzerland

[5]Climate Change Cluster, University of Technology Sydney, Ultimo, NSW 2007, Australia

[6]Department of NanoEngineering, UC San Diego, USA

[7]Marine Biological Research Division, Scripps Institution of Oceanography, UC San Diego, USA

[8]Bioinspired photonics group, Department of Chemistry, University of Cambridge, UK

*Correspondence: dwangpraseurt@ucsd.edu, elena.bollati@bio.ku.dk

Short/running title: Host pigments and light microclimate in corals

Keywords: Symbiosis, photobiology, GFP, optics, fluorescence, photoconversion

Abstract

Pigments homologous to the Green Fluorescent Protein (GFP) have been proposed to fine-tune the internal light microclimate of corals, facilitating photoacclimation of photosynthetic coral symbionts (Symbiodiniaceae) to life in different reef habitats and environmental conditions. However, direct measurements of the *in vivo* light conditions inside the coral tissue supporting this conclusion are lacking. Here, we quantified the intra-tissue spectral light environment of corals expressing GFP-like proteins from widely different light regimes. We focus on (1) photoconvertible red fluorescent proteins (pcRFPs), thought to enhance photosynthesis in mesophotic habitats via wavelength conversion, and (2) chromoproteins (CPs), which provide photoprotection to the symbionts in shallow water via light absorption. Optical microsensor measurements indicated that both pigment groups strongly alter the coral tissue light environment. Estimates derived from light spectra measured in pcRFP-containing corals showed that fluorescence emission can contribute to >50% of orange-red light available to the photosynthetic symbionts at mesophotic depths. We further show that upregulation of pink CPs in shallow-water corals during bleaching leads to a reduction of orange light by 10-20% compared to low-CP tissue. Thus, screening by CPs has an important role in mitigating the light-enhancing effect of coral tissue scattering during bleaching. Our results provide the first experimental quantification of the importance of GFP-like proteins in fine-tuning the light microclimate of corals during photoacclimation.

Introduction

Tropical coral reefs are solar-powered oases of marine biodiversity, where scleractinian corals are responsible for building the reef structures that host over 30% of all named marine multicellular species (Fisher et al., 2015). Corals rely heavily on photosynthesis by their dinoflagellate endosymbionts (Symbiodiniaceae) to meet their metabolic requirements (Muscatine, 1990). The distribution of reef-building corals is therefore constrained by the availability of photosynthetically active radiation (PAR, 400-700 nm), which is in turn determined by physical factors such as latitude, seasonality, water depth and the optical properties of the water body (Kirk, 1994; Kleypas et al., 1999; López-Londoño et al., 2021). Variability in these parameters affects both the quantity and spectral quality of irradiance, exposing corals to a large range of light environments even across small spatial scales (Anthony and Hoegh-Guldberg, 2003; Brakel, 1979; Eyal et al., 2015). On shallow reef flats in clear water regions, corals are routinely exposed to excess irradiance that supersaturates symbiont photosynthesis (Jimenez et al., 2012; Wangpraseurt et al., 2014b), with short light flashes reaching over 3900 µmol photons m^{-2} s^{-1} due to the lensing effect of waves (Veal et al., 2010). Additionally, shallow water corals are exposed to a broad irradiance spectrum covering ultraviolet (UV) to near infrared (NIR) radiation (Wangpraseurt et al., 2014b). At the

other extreme, photosynthetic corals on mesophotic reefs at water depths between 50-150 m can receive as little as 1% of surface PAR, largely concentrated in the blue-green region of the spectrum and greatly reduced for UV and red wavebands (Eyal et al., 2015; Lesser et al., 2009; Tamir et al., 2019). Light conditions can also vary for individual colonies from the same water depth depending on colony morphology (Kaniewska et al., 2011; Wangpraseurt et al., 2014b) and the reef structure that surrounds them (Falkowski and Dubinsky, 1981; Wangpraseurt et al., 2014b).

Corals have evolved a number of mechanisms for optimising symbiont photosynthesis in the presence of spatial and temporal heterogeneity in light availability. Some of these mechanisms occur at the symbiont cell level, while others involve changes in the coral colony morphology and polyp behaviour (Hoogenboom et al., 2008; Kahng et al., 2019; Kaniewska et al., 2014; Kaniewska and Sampayo, 2022; Kramer et al., 2021; Levy et al., 2003; Todd, 2008). Coral symbionts can modify their light harvesting and energy quenching over timescales ranging from seconds to months. For example, non-photochemical quenching allows rapid dissipation of excess irradiance in the photosynthetic apparatus of symbionts, preventing photodamage in high light environments (Einbinder et al., 2016; Gorbunov et al., 2001; Hoegh-Guldberg and Jones, 1999).

Coral symbionts associated with deeper water colonies have been frequently found to differ from their shallow water counterparts in terms of photosystem II photochemical efficiency, maximum electron transport rates, and the organization of light harvesting antennae (Einbinder et al., 2016; Hennige et al., 2008; Lohr et al., 2019).

Photosynthetic pigment concentrations and symbiont cell numbers are dynamic within coral colonies, enabling them to acclimate to changes in irradiance; specifically, corals can increase their symbiont numbers as well as the per cell photosynthetic pigment content in response to a reduction in light levels, and vice versa (Eyal et al., 2019; Falkowski and Dubinsky, 1981; Martinez et al., 2020; Tamir et al., 2020; Titlyanov et al., 2001). Symbiont community composition within colonies is also known to vary along light gradients, although the plasticity of this association and the extent to which it can contribute to photoacclimation appears to be species-specific (Chan et al., 2009; Einbinder et al., 2016; Kaniewska and Sampayo, 2022; Lesser et al., 2010; Martinez et al., 2020; Nir et al., 2011; Winters et al., 2009). Additionally, the interplay between light and temperature is likely to play a role in shaping these communities (Kahng et al., 2019; Kahng and Kelley, 2007), as the low temperatures sometimes encountered on mesophotic reefs affect the photosynthetic rates of symbiont species differently (Grégoire et al., 2017).

Coral host morphology is an important factor controlling the irradiance available for symbiont photosynthesis (Einbinder et al., 2009; Helmuth et al., 1997; Kahng et al., 2019, 2012; Kaniewska et al., 2011; Kaniewska and Sampayo, 2022; Nir et al., 2011; Ralph et al., 2002;

Wangpraseurt et al., 2014b). Coral colonies from low light environments maximize interception with the downwelling irradiance and assume plate-like morphologies that are more conducive to light collection, while shallow water colonies assume self-shading morphologies, such as vertical plates or branches (Anthony et al., 2005; Kaniewska et al., 2011). Morphological adaptations make some species depth-specialists, such as the mesophotic coral *Leptoseris* which can host photosynthetic symbionts down to depths of well over 100 m (Kahng et al., 2020; Rouzé et al., 2021). Depth generalist corals on the other hand, such as *Montastraea cavernosa* in the Caribbean, thrive across light gradients of several orders of magnitude (Lesser et al., 2010). These corals often assume different morphologies in different light environments, allowing a single species to occupy a wider environmental niche; for example, on mesophotic reefs, the depth-generalist corals *Paramontastrea peresi* and *Porites lobata* have growth forms that enhance light exposure and their skeletons have higher reflectivity compared to their shallow water conspecifics, resulting in higher absorption by the symbionts (Kramer et al., 2020). Such morphological differences are partially due to phenotypic plasticity, as shown by transplantation experiments across depth gradients (Muko et al., 2000; Willis, 1985). The relationship between light and colony morphology is not always predictable (Doszpot et al., 2019) as other environmental variables such as hydrodynamics also affect colony morphology (Soto et al., 2019).

Light availability to the coral symbionts depends on the optical properties of the surrounding host tissue and the underlying skeleton (Marcelino et al., 2013; Wangpraseurt et al., 2019, 2012). Coral tissue and skeleton scatter incident light with a strength and directionality that are highly variable across species and even between different structures within a single colony (Enríquez et al., 2017; Marcelino et al., 2013; Wangpraseurt et al., 2019, 2016a). The interplay between tissue and skeleton scattering and reflection and algal absorption modulate coral photosynthesis (Brodersen et al., 2014; Marcelino et al., 2013; Scheufen et al., 2017; Wangpraseurt et al., 2019, 2016a). This can lead to outstanding photosynthetic quantum efficiencies that are close to the theoretical maximum, at least for the coral species for which this parameter has been investigated (Brodersen et al., 2014).

Aside from variability in skeletal morphology, tissue-level changes such as contraction and expansion are known to affect light penetration (Wangpraseurt et al., 2017b, 2014a). The thickness and composition of the tissue can be affected by a number of variables, including genotype, nutritional status, seasonality and environmental history (Harland et al., 1992; Jones et al., 2020; Leinbach et al., 2021; Lough and Barnes, 2000; Rocker et al., 2019). Changes in tissue composition (e.g. lipids, collagen, proteins) will affect the light scattering properties of the bulk tissue (Jacques, 2013), although detailed investigations on coral optical properties in relation to tissue composition and nutrient status remain to be performed (Lyndby et al., 2019).

140 The coral host can also modulate incident light by synthesizing host pigments. The most
141 widespread coral host pigments belong to the Green Fluorescent Protein (GFP)-like
142 superfamily, a group of homologous pigments which are ubiquitous among the Cnidaria
143 (Alieva et al., 2008; Matz et al., 1999; Shimomura et al., 1962). Pigments in this family share
144 a similar structure based on a tripeptide chromophore capable of absorbing visible or UV
145 radiation (Nienhaus and Wiedenmann, 2009). However, despite having similar structure,
146 cnidarian GFP-like proteins exhibit great variability in their optical properties and regulation
147 mechanisms, indicating that they are functionally diverse (Aihara et al., 2019; Alieva et al.,
148 2008; D'Angelo et al., 2008; Leutenegger et al., 2007; Nienhaus and Wiedenmann, 2009;
149 Salih et al., 2000; Smith et al., 2013).
150 GFP-like proteins with inducible expression are found predominantly in corals from high light
151 environments, and they are transcriptionally regulated by blue light intensity (D'Angelo et al.,
152 2008; Salih et al., 2000). GFP-like proteins with light-induced expression include fluorescent
153 proteins (FPs) with emission in the cyan, green and red spectral regions (CFPs, GFPs and
154 RFPs), which absorb light and re-emit it as red-shifted radiation, and non-fluorescent
155 chromoproteins (CPs), which absorb light but have no or little fluorescence emission (Alieva
156 et al., 2008; D'Angelo et al., 2008). These pigments accumulate in high concentration in colony
157 parts with low symbiont densities, often areas of active growth, such as skeletal ridges, the
158 tips of branching corals, the margins of plating corals, and areas affected by epibionts and
159 mechanical damage (D'Angelo et al., 2012; Salih et al., 2000). The increased photon fluxes
160 inside the host tissue caused by the absence of light absorption by the symbionts and light
161 reflection and scattering by skeleton and host tissue components (Enríquez et al., 2005;
162 Wangpraseurt et al., 2017a) have been suggested to cause the high-level pigment expression
163 in these colony parts (Bollati et al., 2020; Smith et al., 2013). Additionally, blue light-induced
164 upregulation as part of an optical feedback loop has been shown to drive strong accumulation
165 of these pigments in bleached corals during episodes of mild heat stress or in heat-free
166 bleaching, caused, for instance, by nutrient stress (Bollati et al., 2020).
167 FPs and CPs with light-induced expression are usually localised ectodermally, and have been
168 shown to exert a photoprotective function on the underlying symbiont layer (Gittins et al., 2015;
169 Quick et al., 2018; Salih et al., 2000; Smith et al., 2013). Upregulation of these pigments in
170 growing parts of colonies and in bleached tissue has been proposed to promote
171 (re)colonisation of host tissue by symbiont cells via the reduction of internal light stress in
172 areas with low symbiont densities (Bollati et al., 2020; D'Angelo et al., 2012; Smith et al.,
173 2013).
174 GFP-like proteins are also widely distributed in corals that are depth generalists or even
175 mesophotic specialists (Eyal et al., 2015; Oswald et al., 2007), where they are constitutively
176 expressed, often at high levels, across a wide range of irradiance regimes (Leutenegger et

al., 2007). It has long been proposed that fluorescent pigments in low light habitats could enhance coral photosynthesis by modulating the spectrum and intensity of light that reaches the symbiont cells (Salih et al., 2000; Schlichter et al., 1994). A light-enhancement mechanism has been suggested for a particular group of constitutive GFP-like proteins known as photoconvertible RFPs (pcRFPs), which are common in thick-tissue depth generalist and mesophotic coral species (Ando et al., 2002; Eyal et al., 2015; Oswald et al., 2007; Wiedenmann et al., 2004). pcRFPs emit green fluorescence when first synthesised, but their chromophores are irreversibly converted to a red-emitting species upon absorption of a UV photon ~390 nm (Ando et al., 2002; Wiedenmann et al., 2004). As coral GFP-like proteins are typically arranged in tetramers, UV-induced post-translational modification leads to the formation of tetramers that contain both green and red subunits; they can therefore absorb light in the blue-green range and re-emit it in the orange-red range via highly efficient Förster Resonance Energy Transfer (FRET) between adjacent subunits (Bollati et al., 2017; Wiedenmann et al., 2004). The orange-red waveband is scarce on mesophotic reefs, yet it can stimulate chlorophyll fluorescence deeper in the tissue compared to blue-green wavelengths because it is poorly absorbed by photosynthetic pigments, an effect analogous to green light driven photosynthesis in plant leaves (de Mooij et al., 2016; Smith et al., 2017; Vogelmann and Evans, 2002). Indeed, pcRFP-containing corals have been shown to survive better under a simulated mesophotic light spectrum as compared to non-pigmented conspecifics (Smith et al., 2017).

While GFP-like proteins are likely to have additional functions for the coral holobiont (Aihara et al., 2019; Ben-Zvi et al., 2022; Id et al., 2021), optimisation of the symbiont light environment is arguably one of their primary roles. The effects of GFP-like proteins on the light environment experienced by coral symbionts are not simply dependent on the spectral properties of the isolated protein; rather, they are a product of the environmental and physiological regulation of the protein within its three-dimensional optical context. For example, microsensor measurements and optical modelling have shown that scattering by GFP-like proteins can enhance light penetration at low GFP concentrations, while high concentrations of GFP increase backscattering and reduce light penetration through the coral tissue (Lyndby et al., 2016; Parkins et al., 2021). Variability in the distribution and arrangement of these proteins – diffuse or granular, ectodermal or endodermal – also affects how they interact with light (Salih et al., 2000; Wangpraseurt et al., 2019), further indicating that spectrally similar GFP-like proteins can be involved in different light modulation mechanisms.

While compelling, the vast majority of evidence provided so far to support the role of GFP-like proteins in modulating the coral photosymbiont light environment during photoacclimation is indirect. This includes light measurements taken outside of the coral tissue (Smith et al., 2017, 2013), optical simulations (Lyndby et al., 2016), and experiments performed on coral-related

214 animals (e.g. corallimorpharians) and isolated symbionts (Smith et al., 2017, 2013). So far,
215 quantitative *in vivo* and *in situ* measurements of the symbiont light environment in response
216 to light-driven changes in host pigment composition have been lacking. Here, we used
217 advanced optical sensor technology to directly quantify how light-driven regulation of GFP-like
218 proteins affects the intra-tissue light microenvironment of depth-generalist and shallow water
219 corals. We focused on the effects of i) UV-driven photoconversion in corals containing
220 pcRFPs, and ii) blue light-driven upregulation of inducible CPs during bleaching and in active
221 growth zones. Our study provides an essential step towards understanding the role of these
222 pigments in optimizing the functioning of the coral-algal symbiosis under extreme light
223 regimes.
224
225 **Results and Discussion**
226 Photoconversion and pcRFPs in depth generalist corals
227 Measurements of scalar irradiance taken at the tissue surface of *M. cavernosa* under white
228 illumination showed an enhancement of 120-180% of the incident irradiance across the visible
229 spectrum. This enhancement was detected in both the unconverted and converted tissue
230 areas measured, with no significant differences between the two in any of the wavebands
231 tested (t-test with Bonferroni adjustment, adjusted $p>0.05$. Figure 1a, Appendix 1—table 1).
232 Vertical light attenuation was strongest between 410-470 nm (covering chlorophyll *a*
233 absorption) and weakest in orange-red wavebands (Figure 1b).
234
235 The enhancement of scalar irradiance commonly observed at the surface of coral colonies is
236 a result of light scattering by the underlying tissue and skeleton (Kühl et al., 1995;
237 Wangpraseurt et al., 2014a), which displays great interspecific variability (Marcelino et al.,
238 2013; Wangpraseurt et al., 2019). Depending on the scattering strength of the two
239 compartments, light in deeper aboral tissue layers can be strongly reduced (Wangpraseurt et
240 al., 2012) or enhanced (Szabó et al., 2014; Wangpraseurt et al., 2020), relative to the top
241 (oral) tissue layers. Our measurements of the tissue attenuation coefficient for *M. cavernosa*
242 indicate shading of the deeper tissue areas, particularly in the violet-blue range (Figure 1b).
243 Additionally, previous measurements of optical scattering suggest that light enhancement due
244 to skeleton backscatter is limited for this species compared to other coral taxa (Marcelino et
245 al., 2013). While these properties may confer bleaching resistance and provide
246 photoprotection for the symbiont population in shallow water (Marcelino et al., 2013;
247 Wangpraseurt et al., 2012), tissue shading greatly reduces carbon fixation rates in symbiont
248 cells found in deeper tissue layers (Wangpraseurt et al., 2016b), which might negatively affect
249 colonies in light-limited environments; yet, *M. cavernosa* is able to thrive at mesophotic depths
250 (Lesser et al., 2010).

At the coral surface, spectral changes due to conversion of the pcRFP pool were observed at the absorption and emission peaks of the green (507 and 514 nm) and red chromophore (571 and 582 nm) (Figure 1a). Surface light enhancement by GFP-like proteins in corals can be attributed to a combination of elastic scattering (i.e. scattering without modifications of photon energy) and inelastic scattering (i.e. scattering with modification of photon energy, such as the case of absorption followed by fluorescence emission) (Lyndby et al., 2016). Under white light, the degree of photoconversion of the pcRFP pool did not appear to significantly affect the spectral attenuation coefficient (Figure 1b), indicating that the effects of pcRFP scattering on attenuation of the incident are relatively small compared to the effects of tissue scattering and photosynthetic pigment absorption. Therefore it appears that, for this pcRFP-containing coral specimen, host pigment-derived enhancement of light would be a minor component for the overall tissue light microclimate in a shallow water environment, albeit with some variability due to water depth and the optical properties of the water column, as well as spectral differences between our white measuring light and sunlight. In contrast, corals on mesophotic reefs experience a much more narrow incident spectrum, where blue-green wavelengths that efficiently excite pcRFPs are abundant, while light in the orange-red spectral range is greatly reduced (Eyal et al., 2015; Lesser et al., 2009; Tamir et al., 2019). Under these conditions, the relative contributions of light scattering and fluorescence emission by pcRFPs are therefore likely very different from those measured under white light.

To isolate the contribution of fluorescence emission by the pcRFP pool to the tissue light microenvironment of *M. cavernosa*, we collected fluorescence emission profiles in the 505-700 nm range using a blue (455-505 nm) excitation light source (Figure 2, Figure 2—figure supplement 1). The peak emission wavelength of this light source matches (± 3 nm) the irradiance maximum measured at 80 m depth in the Red Sea (Eyal et al., 2015), and over 50% of irradiance at 80m falls within the 455-505 nm band (Figure 2—figure supplement 1). Therefore, while not a perfect match, this light source is spectrally more representative of mesophotic light conditions compared to the broad-spectrum LED (Figure 2—figure supplement 1). As a proxy for the degree of photoconversion, we used the ratio of 514:582 nm emission measured at the coral surface. This ratio was significantly higher in *unconverted* corals, compared to those that had been exposed to UV light (Figure 2—figure supplement 2) for any duration (*partially converted* or *converted* corals, Two-way ANOVA followed by Tukey's post-hoc test, adjusted $p < 0.01$. Figure 2, Appendix 1—table 2). The ratio showed a significant decrease from surface to 350 μm tissue depth only for *unconverted* corals (adjusted $p < 0.01$), and no significant differences were detected between the two groups at 350 μm tissue depth (adjusted $p > 0.05$).

286 These results indicate that attenuation of light emitted by the unconverted chromophore is
287 more pronounced relative to attenuation of the converted chromophore emission (Figure 2a,c).
288 This is in agreement with the white light attenuation coefficient (Figure 1b), which was weaker
289 in the orange-red range. The peridinin-chlorophyll *a*-protein (PCP) light harvesting complex
290 efficiently absorbs blue, green and red wavelengths (Jiang et al., 2012), resulting in strong
291 attenuation by symbionts in the oral gastrodermis (Figure 1); conversely, poor absorption of
292 orange light by symbiont pigments allows this waveband to penetrate deeper into the tissue
293 (Figure 1) (Lichtenberg et al., 2016).
294
295 Using isolated symbionts and the sea anemone *Discosoma* as model systems for the
296 symbiosis between cnidarian and Symbiodiniaceae, Smith et al. (2017) showed that orange
297 light has a higher potential to stimulate photosynthesis in symbiont cells found deeper in the
298 tissue as compared to blue-green light. This effect is analogous to what is observed in plant
299 leaves, where enhanced illumination with green light increases photosynthesis in deeper cell
300 layers (de Mooij et al., 2016; Vogelmann and Evans, 2002). Therefore, based on this indirect
301 evidence it was proposed that orange fluorescence emission by pcRFPs could provide an
302 energetic advantage for symbiotic corals in greater water depths dominated by blue light
303 (Smith et al., 2017). Indeed, colour morphs with pcRFPs survived longer than non-pigmented
304 conspecifics in simulated deep water light environments (Smith et al., 2017).
305 In this study, we aimed to directly measure the impact of pcRFPs on the in hospite light
306 environment experienced by algal symbionts in coral tissue. We used the blue light excited
307 fluorescence emission profiles from *M. cavernosa* (Figure 2c) at different stages of
308 photoconversion (Figure 3a-c) to calculate the number of photons generated by fluorescence
309 emission integrated over the green (Figure 3d) and red (Figure 3e) spectral range.
310 Fluorescence emission by the pcRFP pool in the most converted state provided an amount of
311 orange-red photons that ranged between 1% (close to the skeleton) and 5% (at the coral
312 surface) of the incident blue irradiance, with intermediate values of around 3% at a tissue
313 depth of 400 μm (Figure 3e). This direct measurement demonstrates that orange-red
314 fluorescence from host pigments penetrates well in coral tissue. Furthermore, these values
315 show that ectodermal pcRFPs can improve the illumination of deeper tissue layers exposed
316 to the narrow mesophotic light spectrum. Thus, under a mesophotic light spectrum, the
317 symbionts harboured by conspecific fluorescent morphs experience a spectrally different light
318 environment depending on the pigment complement expressed by their host (Ben-Zvi et al.,
319 2021). We obtained a similar result for a second species, *Echinophyllia* sp., by comparing
320 specimens that contain a highly converted pcRFP to conspecific morphs that contain GFP but
321 lack pcRFPs entirely (Figure 3—figure supplement 1). This confirms the relevance of our
322 findings to other pcRFP-containing corals from mesophotic environments (Eyal et al., 2015).

323

324 To predict how spectral modifications by pcRFPs affect *in situ* light harvesting on mesophotic
325 reefs, we used a published dataset of downwelling spectral irradiance from a coral reef in Eilat
326 (Eyal et al., 2015) (Figure 4a) and simulated the *in vivo* emission of orange-red light along a
327 depth gradient from 10 to 130 m, using the *converted M. cavernosa* as a model (Figure 4b).
328 The incident 455-505 nm light required to excite the pcRFP pool is relatively abundant down
329 to 100 m water depth (1.5 μmol photos m^{-2} s^{-1}), however the amount of 560-650 nm light is
330 only in the range of 1 μmol photons m^{-2} s^{-1} at 50 m and attenuates rapidly to about 0.1 μmol
331 photons m^{-2} s^{-1} at 80 m (Figure 4a). As a consequence, the pcRFP pool between 50 and 80
332 m depth can effectively double the scalar irradiance in the 560-650 nm waveband compared
333 to corals without pcRFPs (Figure 4b). On mesophotic reefs beyond 80 m water depth,
334 simulated fluorescence emission by the pcRFP becomes the dominant source of 560-650 nm
335 light for this *M. cavernosa* specimen. This calculation yielded similar results when applied to
336 a dataset of modelled irradiance in the Bahamas (Lesser et al., 2009) (Figure 4—figure
337 supplement 1), a natural habitat of this species, suggesting that our findings are relevant to
338 mesophotic reef systems independent from potential differences in the underwater light
339 environment.
340 We note that our analysis could lead to overestimation of predicted red fluorescence at shallow
341 depths, where high light levels may theoretically excite the entire chromophore population thus
342 resulting in a non-linear relationship between incident light and fluorescence emission.
343 However, the relationship between fluorescence emission and excitation light was linear up to
344 at least 20 μmol photons m^{-2} s^{-1} of incident 455-505 nm light, the maximum intensity reached
345 in our calibration measurements (Appendix 1, Appendix 1—figure 1, Appendix 1—table 3),
346 corresponding to the incident irradiance (455-505 nm) measured at 48 m depth in the Red
347 Sea (Figure 4a). Our calculations of fluorescence emission were thus considered accurate
348 below 48 m water depth.
349
350 Even though this constitutes a dramatic spectral alteration in relative terms, it is important to
351 note that 1) the absolute number of photons generated by pcRFP fluorescence is small
352 compared to what is provided by ambient light in shallow waters and 2) the *in hospite*
353 irradiance is still dominated by the blue-green spectrum, which should be regarded as the
354 main source of irradiance for coral symbionts in the mesophotic zone. Thus, under conditions
355 of high solar radiation, the benefit of pcRFP fluorescence for photosynthesis may be negligible
356 compared to the potential energetic investments related to maintaining a dense pcRFP
357 pigment pool (Leutenegger et al., 2007; Oswald et al., 2007; Quick et al., 2018). However,
358 under strong light-limitation (<40 μmol photons m^{-2} s^{-1}) pcRFP-driven photosynthesis might be
359 energetically advantageous, as suggested by the increased long term survival of pcRFP-

360 containing coral morphs compared to their brown conspecifics under mesophotic light regimes
361 (Smith et al., 2017). Such small fitness advantage could have contributed as a driving factor
362 in some of the multiple instances of convergent evolution of red emitting homologues from
363 green ancestor proteins (Field et al., 2006; Gittins et al., 2015; Shagin et al., 2004; Ugalde et
364 al., 2004). Furthermore, the benefits and trade-offs associated with high level expression of
365 pcRFPs may have contributed to the rise of colour morphs among individuals from genera
366 such as *Trachyphyllia, Lobophyllia, Echinophyllia* and *Montastraea* (Field et al., 2006; Gittins
367 et al., 2015; Oswald et al., 2007) as a result of balancing selection as previously suggested
368 for GFP-like proteins in both shallow and deep water corals (Quick et al., 2018).
369 It is important to note that host pigments are only one of many variables that influence the
370 optical properties of coral colonies along a depth gradient. For *M. cavernosa*, one study
371 reported differences in skeletal microstructure between colonies collected from different
372 depths (Beltrán-Torres and Carricart-Ganivet, 1993). Another study revealed a shift towards
373 heterotrophy and a change in symbiont community composition for the same species along a
374 shallow to mesophotic gradient (Lesser et al., 2010). Genetic structuring of the *M. cavernosa*
375 population with depth has also been reported (Brazeau et al., 2013). All these variables can
376 potentially affect bio-optical properties and/or photosynthesis, and thus affect the success of
377 this species across steep light gradients. In this study, we controlled for these variables by
378 choosing to perform our measurements on clonal replicates from long-term aquarium culture.
379 This approach allows us to confidently attribute the measured changes in internal light
380 environment to the changes in the pcRFP complement that we induced experimentally.
381 Further studies are welcome to analyse if and how other variables may interact with pcRFPs
382 functions to shape the symbiont light environment along natural depth gradients. Finally,
383 intraspecific colour polymorphism of reef corals is frequently driven by different tissue
384 concentrations of GFP-like proteins including CPs and pcRFPs (Gittins et al., 2015; Quick et
385 al., 2018; Smith et al., 2017). Accordingly, representatives of different colour morphs can be
386 expected to show deviating responses.
387
388 <u>Photoprotective chromoproteins and bleaching in shallow water corals</u>
389 To evaluate the effect of high ectodermal concentrations of CPs on the light environment of
390 coral symbionts *in hospite*, we performed spectral scalar irradiance measurements on
391 colonies of *Pocillopora damicornis* and *Montipora foliosa*. Pink colour morphs of *P. damicornis*
392 express a CP with absorption maximum at 565 nm (Dove et al., 1995), which can accumulate
393 in high concentrations following bleaching (Bollati et al., 2020) (Figure 5a). Brown morphs of
394 this species do not produce detectable amounts of CP, although they contain a CFP (Figure
395 5a). The bare white skeleton of *P. damicornis* enhanced spectral scalar irradiance by 140-
396 150% across the entire visible spectrum (Figure 5b). In brown morphs, the enhancement was

397 reduced to <120% in the wavebands corresponding to the absorption peaks of symbiont
398 photosynthetic pigments, while the enhancement remained close to 130% in the orange region
399 of the spectrum (Figure 5a). Bleached corals expressing high pink CP concentrations
400 experienced a surface light enhancement in the blue spectral region comparable to what was
401 measured over bare skeleton; however, this was reduced to ~123% in the orange waveband
402 corresponding to the absorption peak of the CP (Figure 5b). Measurements of the spectral
403 attenuation coefficient from colony surface to skeleton showed that brown unbleached tissue
404 is light-attenuating in the blue and red regions of photosynthetic pigment absorption, but light-
405 enhancing in the orange-red region; conversely, blue and red light are enhanced in bleached
406 pink tissue, while orange light is attenuated (Figure 5c).
407 *M. foliosa* has several colour morphs, one of which produces high concentrations of a purple
408 CP localised in areas of low symbiont density at the colony margins, while the inner area has
409 low CP content and appears brown (D'Angelo et al., 2012) (Figure 5d). Measurements of
410 surface spectral scalar irradiance on tissue found in the inner region of the colony showed
411 similar spectral properties to those of brown *P. damicornis* and exhibited 140% light
412 enhancement, which was reduced to 110% in the symbiont photosynthetic pigments
413 absorption wavebands (Figure 5e). In the high CP area at the colony margin, scalar irradiance
414 showed a strong enhancement (>150%) comparable to what measured for bleached tissue in
415 a CP-free morph (Figure 5e); however, this was heavily spectrally modified by the presence
416 of the purple CP, which reduced light enhancement by up to 25% within its absorption
417 spectrum compared to other spectral bands (Figure 5e). Screening by CPs via absorption was
418 proposed as a photoprotective mechanisms in shallow water corals by Smith et al. (2013),
419 who used external reflectance measurements as well as measurements on freshly isolated
420 symbionts in seawater to provide indirect support for their hypothesis. Our data thus provide
421 the first direct evidence that coral CPs do indeed reduce light penetration within their
422 absorption spectrum, dramatically altering the *in hospite* light environment of coral symbionts.
423 The *P. damicornis* skeleton exhibits an intermediate level of microscale fractality and an
424 intermediate scattering coefficient (mass-fractal dimension ~1.75 and reduced scattering
425 coefficient of ~7.5 mm^{-1} (Marcelino et al., 2013)), which implies a relatively efficient
426 redistribution of light over the tissue (Marcelino et al., 2013). While this type of skeletal
427 structure can help healthy corals optimise photosynthesis, during bleaching this can amplify
428 the irradiance increase derived from the loss of photosynthetic pigment absorption (Enríquez
429 et al., 2005; Marcelino et al., 2013; Wangpraseurt et al., 2017a). Our data confirms that
430 bleached *P. damicornis* tissue indeed experiences a strongly light enhancing
431 microenvironment, resulting from enhanced skeletal scattering due to reduced tissue
432 absorption (Wangpraseurt et al., 2017a). Such strongly enhanced light microhabitat can also
433 be found in healthy corals such as in the growing plate margins of *M. foliosa*, where the

434 symbiont population is less abundant compared to the inner areas (Figure 5d). While blue light
435 is attenuated in unbleached corals, the absence of symbionts in bleached corals or tissue
436 areas with low symbiont densities (e.g. in areas of active tissue growth), results in the
437 enhancement of blue light possibly leading to transcriptional upregulation of CPs (D'Angelo et
438 al., 2008). This supports the notion that the optical feedback loop is a key mechanism
439 underlying the colourful bleaching phenomenon (Bollati et al., 2020). Our data also shows that
440 high CP concentrations counteract the light-enhancing effects of bleaching within the CP
441 absorption spectrum, as signified by the relative light enhancement measured in bleached
442 corals in the orange region, a waveband known to result in light stress and bleaching for
443 various coral species when provided at high irradiance (Quick et al., 2018; Smith et al., 2013;
444 Wijgerde et al., 2014). Thus, optimisation of the light microenvironment by CPs in symbiont-
445 depleted tissue could provide the necessary conditions for (re) colonisation by symbiont cells
446 (Bollati et al., 2020; D'Angelo et al., 2012; Smith et al., 2013).

447 **Orange-red light: a double-edged sword for coral holobionts**
448 The data presented in this study clearly show that light-driven regulation of GFP-like host
449 pigments can result in fine spectral tuning of the intra-tissue light field of corals. The pcRFPs
450 and CPs examined here are characterised by very different optical properties, environmental
451 regulation and ecological distribution, however they share a commonality in that both types
452 of pigment regulate internal light fluxes in the orange-red spectral range. Enhancement of
453 this waveband may be a double-edged sword for corals; on one hand, poor absorption by
454 photosynthetic pigments allows better penetration (Smith et al., 2017), which can be
455 exploited by pcRFP-containing corals to illuminate deeper tissue areas under light limitation.
456 On the other hand, light amplification in symbiont-free tissue produces excess irradiance in
457 the same waveband, which can cause photodamage unless counteracted by CP screening
458 or other photoprotective mechanisms (Quick et al., 2018; Smith et al., 2013; Wangpraseurt
459 et al., 2017a; Wijgerde et al., 2014). While our study has demonstrated the effects of host
460 pigment regulation on the availability of orange-red light to the symbiont, the symbiont
461 response to this spectral alteration remains to be demonstrated *in hospite* and quantified in
462 terms of photosynthetic production. To date, very few studies have explored the effects of a
463 red-shifted spectrum on symbiont photobiology *in hospite* (Lichtenberg et al., 2016; Szabó et
464 al., 2014; Wangpraseurt et al., 2014c). The available data suggests that red illumination can
465 support similar levels of photosynthetic production in deeper tissue areas compared to
466 shallow ones, despite reduced light availability deeper in the tissue (Lichtenberg et al.,
467 2016). Similar rates of oxygen evolution were also observed *in hospite* for symbionts
468 exposed to either blue-shifted or red-shifted broad illumination, however under low light
469 conditions red-shifted illumination resulted in lower electron transport rates (Wangpraseurt et
470 al., 2014c). Finally, in cultured coral symbionts, the absorption cross-section of PSII is over
471 3x higher in the blue region compared to the orange-red, however this difference becomes
472 less pronounced when the symbionts are studied *in hospite* (Szabó et al., 2014). A more
473 complete understanding of how coral symbionts acclimate to and utilise orange-red light *in*
474 *hospite* is clearly needed in order to understand how spectral tuning of this waveband by
475 host pigments impacts holobiont photosynthesis.
476
477
478
479 **Materials and Methods**
480 Coral culture and aquarium set up
481 Coral colonies of *M. cavernosa* (one genet, three ramets), *Echinophyllia* sp. (two genets, one
482 ramet of each), *Pocillopora damicornis* (two genets, one ramet) and *Montipora foliosa* (two
483 genets, one ramet of each) were asexually propagated for >10 years in the experimental coral

484 aquarium facility of the Coral Reef Laboratory, National Oceanography Centre, Southampton,
485 UK (D'Angelo and Wiedenmann 2012b). Each sample represents an autonomous colony with
486 an individual, long-term growth history. Therefore, while genetically identical, these samples
487 can be considered true biological replicates. These species and colour morphs were selected
488 for their established production of pcRFPs (*M. cavernosa* and *Echinophyllia* sp.) or
489 photoprotective CPs (*P. damicornis* and *M. foliosa*) (Bollati et al., 2020; D'Angelo et al., 2012;
490 Eyal et al., 2015; Oswald et al., 2007). Additionally, their very long-term growth and
491 propagation in our stable aquarium conditions ensured that these individuals were fully
492 acclimated to the pre-experimental conditions, thus allowing to ascribe any observed patterns
493 exclusively to the manipulated parameters – something that would not be straightforward for
494 field collected or recently acquired colonies.
495 All corals were acclimated for >6 months to the light conditions specified in Appendix 1—table
496 4, at a temperature of ~25°C, salinity 31, and were fed twice weekly with rotifers. Nutrient
497 levels were maintained around ~6.5μM nitrate and ~0.3 μM phosphate (D'Angelo and
498 Wiedenmann 2012b; Wiedenmann et al. 2013) unless otherwise specified in the text and in
499 Appendix 1—table 4. A detailed description of the aquarium set up including flow rates,
500 volumes, co-cultured species and monitoring of environmental parameters is presented in
501 (D'Angelo and Wiedenmann 2012b).
502
503 Spectral scalar irradiance measurements
504 Microscale spectral light measurements were conducted as described in Wangpraseurt et al.
505 (2017a) using scalar irradiance microsensors with a spherical tip diameter of 60 µm (Rickelt
506 et al., 2016) and connected to a fiber-optic spectrometer (QE65000, Ocean Optics, USA).
507 Microsensor profiles were performed from the coral skeleton upwards towards the tissue
508 surface in vertical increments of 20-100 µm using a motorized micromanipulator (Pyroscience
509 GmbH, Germany) controlled by dedicated software (Profix, Pyroscience GmbH, Germany).
510 The step size was adjusted according to the total coral tissue thickness with step sizes of 20
511 µm for *P. damicornis* (tissue thickness ~150-300 µm), 70 µm for *M. cavernosa* (tissue
512 thickness 400-800 µm) and *Echinophyllia* (tissue thickness 900 µm). For *M. foliosa*, only
513 surface spectra were collected as the tissue was very thin (< 60 µm). Scalar irradiance
514 measurements were performed using vertical illumination from above, while the scalar
515 irradiance microsensor was inserted into coral tissue at an angle of 45° relative to the incident
516 light (Figure 2—figure supplement 1 a). This measurement geometry was chosen to minimise
517 artificial shading of the sensor tip while still allowing sensor penetration to the full tissue depth
518 (Rickelt et al., 2016; Wangpraseurt et al., 2012). White LED illumination was provided by a
519 fiber-optic lamp (KL-1600 LED, Schott GmbH, Germany) (Figure 2—figure supplement 1 a,b),
520 producing 360-900 μmol photons m^{-2} s^{-1} at the measurement distance.

521 For *M. cavernosa* and *Echinophyllia*, we also measured the spatial distribution of emitted
522 fluorescence. For this, narrow-waveband excitation in the blue spectral range was provided
523 vertically incident by a xenon arc lamp equipped with a band-pass filter (Leica GFPplus filter,
524 λ=455-505nm, Figure 2—figure supplement 1 c) and scalar irradiance measurements in the
525 505-650 nm range were used to estimate fluorescence emission. The light source output (455-
526 505 nm) at the measurement distance was 12-46 μmol photons m^{-2} s^{-1}. No emission filter was
527 used on the detector side as bleed-through of excitation light in this spectral range was minimal
528 (<0.5%).
529 Scalar irradiance microsensor measurements were calibrated against a spectroradiometer
530 (MSC15, Gigahertz-Optik, Germany) by measuring the incident downwelling irradiance from
531 the white LED light source over a black light absorbing surface first with the microsensor in
532 water, then with the spectroradiometer at the same distance from the light source in air
533 (Brodersen et al., 2014; Wangpraseurt et al., 2012).
534
535 Induction of photoconversion and measurements of pcRFP-containing corals
536 We performed scalar irradiance measurements in *M. cavernosa* at different stages of
537 photoconversion to assess how UV driven photoconversion of the pcRFP pool affects the
538 symbiont light environment. We defined the stages of photoconversion by the relative
539 proportions of green (514 nm) and red (582 nm) fluorescence emission, measured with 455-
540 505 nm excitation at the colony surface. A 514:582 nm ratio >1 indicates a higher contribution
541 of the green chromophore (defined as *unconverted* coral), a ratio ~1 indicates substantial
542 contributions from both the green and the red chromophore (defined as *partially converted*
543 coral), and a ratio <1 indicates a higher contribution of the red chromophore (defined as
544 *converted* coral).
545 To obtain *unconverted* corals, we placed two colonies derived from fragmentation of the same
546 mother colony under green incident irradiance provided by LED strips (Lumiled Luxeon Rebel
547 Green, λ=530 nm, FWHM=60 nm; Figure 2—figure supplement 2 a) for 40 days. This
548 treatment resulted in the accumulation of the unconverted pcRFP (Leutenegger et al., 2007),
549 evidenced by a 514:582 nm emission ratio >1. We then used one of these colonies to induce
550 localised photoconversion by illuminating the coral tissue surface (spot diameter 3 mm) with
551 a xenon arc lamp of a fluorescence microscope (Leica MZ10 equipped with a UV bandpass
552 filter (λ=355 nm, FWHM=55 nm; Figure 2—figure supplement 2 b) for 6 hours (Eyal et al.,
553 2015); this waveband only partially overlaps with the action spectrum of pcRFP
554 photoconversion (Wiedenmann et al., 2004) and is therefore less effective in inducing the
555 photochemical reaction. In combination with the limited duration of the exposure, the UV
556 treatment resulted in a mix of unconverted and converted pcRFP, as evidenced from the

557 514:582 nm ratio ~1 (*partially converted* coral). The second *M. cavernosa* colony was exposed
558 to near-UV irradiance provided by LED strips (Aquaray NUV, λ=412, FWHM=18.5 nm; Figure
559 2—figure supplement 2 c) for 10 hours; this treatment induces rapid photoconversion of the
560 pcRFP pool (Bollati et al., 2017), resulting in a 514:582 nm emission ratio <1 (*converted* coral).
561 All photoconversion experiments were performed in a flow-through system at a water
562 temperature of 26°C regulated by a 25 W aquarium heater (Tunze).
563 We also assessed the contribution of fluorescence emission by pcRFPs to spectral scalar
564 irradiance against other GFP-like proteins by performing measurements on two morphs of
565 *Echinophyllia* sp.. Both morphs had been kept under broad spectrum illumination long term,
566 side by side in our mesocosm. The green morph contained a non-inducible GFP, while the
567 red morph contained a CFP and a highly converted pcRFP (green:red emission ratio <<1)
568 (Alieva et al., 2008; Bollati et al., 2017; Smith et al., 2017).
569
570 Experimental bleaching and measurements of corals containing inducible CPs
571 To test how bleaching affects irradiance in corals containing inducible CPs, we performed
572 measurements on one healthy and one bleached individual each of *P. damicornis* and *M.*
573 *foliosa* (3 replicate measurements per sample per condition). A *P. damicornis* colour morph
574 capable of expressing a pink CP with absorption maximum at 565 nm (Bollati et al., 2020;
575 D'Angelo et al., 2008; Dove et al., 1995) was bleached by exposure to 400 μmol photons m^{-2}
576 s^{-1} of red LED light (Lumiled Luxeon Rebel Deep Red, λ=660 nm, FWHM=40 nm; Figure 2—
577 figure supplement 2 d) for 7 days. This treatment induces bleaching without inducing the
578 expression of the light-sensitive genes responsible for CP production (Bollati et al., 2020;
579 D'Angelo et al., 2008; Smith et al., 2013; Wijgerde et al., 2014). Bleaching was confirmed by
580 visual comparison with >10 untreated specimens, which were kept in a separate area of the
581 same aquarium under broad illumination from a metal halide lamp. Bleached fragments were
582 then exposed to blue light (100 μmol photons m^{-2} s^{-1}; Lumiled Luxeon Rebel Royal Blue, λ=450
583 nm, FWHM=40 nm; Figure 2—figure supplement 2 e) for 20 days to stimulate upregulation of
584 the pink CP, resulting in a "colourful bleaching" response (Bollati et al., 2020; D'Angelo et al.,
585 2008) (Figure 2—figure supplement 2). Alongside the bleached specimen, we performed
586 spectral scalar irradiance measurements on i) a *P. damicornis* skeleton and ii) an unbleached
587 brown morph of the same species, which expresses an inducible CFP but no CP.
588 For *M. foliosa*, we measured a morph capable of producing a CFP and a pink CP, with the
589 latter accumulating in high concentrations at the colony margins (Bollati et al., 2020; D'Angelo
590 et al., 2012). We compared this healthy, unbleached coral with a *M. foliosa* morph that does
591 not produce CPs, bleached by phosphate starvation (Bollati et al., 2020; Rosset et al., 2017;
592 Wiedenmann et al., 2013) after 65 days in our high nitrate / low phosphate mesocosm

(D'Angelo and Wiedenmann 2012a). Both colonies were kept under broad spectrum illumination (200 μmol photons m^{-2} s^{-1}; Aquamedic metal halide lamp).

Data processing

All spectral data were corrected for spectrometer dark noise readings obtained under dark conditions and calibrated against a spectroradiometer as described above. For spectral measurements performed under incident white light, the spectra were normalised to the incident irradiance as described previously (Wangpraseurt et al., 2012).

The spectral attenuation coefficient of scalar irradiance ($K_0(\lambda)$) was calculated from measurements obtained under white light following Kühl (2005):

$$K_0(\lambda) = \frac{\ln\left(\frac{E_0(\lambda)_1}{E_0(\lambda)_2}\right)}{z_2 - z_1}$$

where $E_0(\lambda)_1$ and $E_0(\lambda)_2$ are the spectral scalar irradiance measured at tissue depths z_1 and z_2. $K_0(\lambda)$ was calculated from surface to skeleton using the average tissue thickness (deduced from the mean number of equal steps performed by the micromanipulator from the skeleton to the upper tissue surface: 560 μm for *M. cavernosa*, 300 μm for *P. damicornis*).

For fluorescence emission measurements under blue excitation, integrated photon irradiance was calculated for different portions of the visible spectrum (incident: 455-505 nm; green emission: 505-560 nm; red emission: 560-650 nm) after converting spectral scalar irradiance to spectral photon scalar irradiance using Plancks equation (see Lichtenberg et al. (2017)). Integrated photon irradiance over the same incident (455-505 nm) and red (560-650 nm) spectral ranges was also calculated for a dataset of field spectral scalar irradiance collected from Eilat, Israel (Eyal et al., 2015) and for a dataset of spectral scalar irradiance simulated from surface measurements collected in the Bahamas (Lesser et al., 2009). These values were used to calculate estimates of red fluorescence emission for the *converted M. cavernosa* at different water depths, by multiplying the integral of the 455-505 nm field radiance by the percentage of incident light re-emitted as 560-650 nm fluorescence shown in Figure 3e.

Acknowledgements

This project was supported by the European Union's Horizon 2020 research and innovation programme (702911-BioMIC-FUEL, D.W.), the Gordon and Betty More Foundation (grant GBM 9325 to D.W. & grant GBMF9206 https://doi.org/10.37807/GBMF9206 to MK) and the Natural Environment Research Council (grant number NE/S003533/2 to JW and CDA).

Data availability

Data used in this study is available from https://doi.org/10.5061/dryad.0gb5mkm1z

References

Aihara Y, Maruyama S, Baird AH, Iguchi A, Takahashi S, Minagawa J. 2019. Green fluorescence from cnidarian hosts attracts symbiotic algae. *Proceedings of the National Academy of Sciences* **116**:2118–2123. doi:10.1073/pnas.1812257116

Alieva NO, Konzen KA, Field SF, Meleshkevitch EA, Hunt ME, Beltran-Ramirez V, Miller DJ, Wiedenmann J, Salih A, Matz M V. 2008. Diversity and evolution of coral fluorescent proteins. *PLoS ONE* **3**:e2680. doi:10.1371/journal.pone.0002680

Ando R, Hama H, Yamamoto-Hino M, Mizuno H, Miyawaki A. 2002. An optical marker based on the UV-induced green-to-red photoconversion of a fluorescent protein. *Proceedings of the National Academy of Sciences* **99**:12651–12656. doi:10.1073/pnas.202320599

Anthony KRN, Hoegh-Guldberg O. 2003. Variation in coral photosynthesis, respiration and growth characteristics in contrasting light microhabitats: An analogue to plants in forest gaps and understoreys? *Functional Ecology* **17**:246–259. doi:10.1046/j.1365-2435.2003.00731.x

Anthony KRN, Hoogenboom MO, Connolly SR. 2005. Adaptive variation in coral geometry and the optimization of internal colony light climates. *Functional Ecology* **19**:17–26. doi:10.1111/j.0269-8463.2005.00925.x

Beltrán-Torres AU, Carricart-Ganivet JP. 1993. Skeletal morphologic variation in *Montastrea cavernosa*. *Revista de Biología Tropical* **41**:559–562.

Ben-Zvi O, Lindemann Y, Eyal G, Loya Y. 2022. Coral fluorescence: a prey-lure in deep habitats. *Communications Biology* **5**:537. doi:10.1038/s42003-022-03460-3

Ben-Zvi O, Wangpraseurt D, Bronstein O, Eyal G, Loya Y. 2021. Photosynthesis and bio-optical properties of fluorescent mesophotic corals. *Front Mar Sci* **8**:1–12. doi:10.3389/fmars.2021.651601

Bollati E, D'Angelo C, Alderdice R, Pratchett M, Ziegler M, Wiedenmann J. 2020. Optical feedback loop involving dinoflagellate symbiont and scleractinian host drives colorful coral bleaching. *Current Biology* **30**:1–13. doi:10.1016/j.cub.2020.04.055

Bollati E, Plimmer D, D'Angelo C, Wiedenmann J. 2017. FRET-mediated long-range wavelength transformation by photoconvertible fluorescent proteins as an efficient mechanism to generate orange-red light in symbiotic deep water corals. *International Journal of Molecular Sciences* **18**:1174. doi:10.3390/ijms18071174

Brakel W. 1979. Small-scale spatial variation in light available to coral reef benthos: Quantum irradiance measurements from a Jamaican reef. *Bulletin of Marine Science* **29**:406–413.

Brazeau DA, Lesser MP, Slattery M. 2013. Genetic Structure in the Coral, Montastraea cavernosa: Assessing Genetic Differentiation among and within Mesophotic Reefs. *PLoS ONE* **8**. doi:10.1371/journal.pone.0065845

Brodersen KE, Lichtenberg M, Ralph PJ, Kühl M, Wangpraseurt D. 2014. Radiative energy budget reveals high photosynthetic efficiency in symbiont-bearing corals. *Journal of the Royal Society Interface* **11**:20130997. doi:10.1098/rsif.2013.0997

Chan YL, Pochon X, Fisher MA, Wagner D, Concepcion GT, Kahng SE, Toonen RJ, Gates RD. 2009. Generalist dinoflagellate endosymbionts and host genotype diversity detected from mesophotic (67-100 m depths) coral *Leptoseris*. *BMC Ecology* **9**. doi:10.1186/1472-6785-9-21

D'Angelo C, Denzel A, Vogt A, Matz M V., Oswald F, Salih A, Nienhaus GU, Wiedenmann J. 2008. Blue light regulation of host pigment in reef-building corals. *Marine Ecology Progress Series* **364**:97–106. doi:10.3354/meps07588

D'Angelo C, Smith EG, Oswald F, Burt J, Tchernov D, Wiedenmann J. 2012. Locally accelerated growth is part of the innate immune response and repair mechanisms in reef-building corals as detected by green fluorescent protein (GFP)-like pigments. *Coral Reefs* **31**:1045–1056. doi:10.1007/s00338-012-0926-8

D'Angelo C, Wiedenmann J. 2012a. An experimental mesocosm for long-term studies of reef corals. *Journal of the Marine Biological Association of the United Kingdom* **92**:769–775. doi:10.1017/S0025315411001883

D'Angelo C, Wiedenmann J. 2012b. An experimental mesocosm for long-term studies of reef corals. *Journal of the Marine Biological Association of the United Kingdom* **92**:769–775. doi:doi:10.1017/S0025315411001883

de Mooij T, de Vries G, Latsos C, Wijffels RH, Janssen M. 2016. Impact of light color on photobioreactor productivity. *Algal Research* **15**:32–42. doi:10.1016/j.algal.2016.01.015

Doszpot NE, McWilliam MJ, Pratchett MS, Hoey AS, Figueira WF. 2019. Plasticity in three-dimensional geometry of branching corals along a cross-shelf gradient. *Diversity (Basel)* **11**. doi:10.3390/D11030044

Dove SG, Takabayashi M, Hoegh-Guldberg O. 1995. Isolation and partial characterization of the pink and blue pigments of pocilloporid and acroporid corals. *The Biological Bulletin* **189**:288–297. doi:10.2307/1542146

Einbinder S, Gruber DF, Salomon E, Liran O, Keren N, Tchernov D. 2016. Novel adaptive photosynthetic characteristics of mesophotic symbiotic microalgae within the reef-building coral, *Stylophora pistillata*. *Front Mar Sci* **3**. doi:10.3389/fmars.2016.00195

Einbinder S, Mass T, Brokovich E, Dubinsky Z, Erez J, Tchernov D. 2009. Changes in morphology and diet of the coral *Stylophora pistillata* along a depth gradient. *Marine Ecology Progress Series* **381**:167–174.

Enríquez S, Méndez ER, Hoegh-Guldberg O, Iglesias-Prieto R. 2017. Key functional role of the optical properties of coral skeletons in coral ecology and evolution. *Proceedings of the Royal Society of London B: Biological Sciences* **284**. doi:10.1098/rspb.2016.1667

Enríquez S, Méndez ER, Iglesias-Prieto R. 2005. Multiple scattering on coral skeletons enhances light absorption by symbiotic algae. *Limnology and Oceanography* **50**:1025–1032. doi:10.4319/lo.2005.50.4.1025

Eyal G, Cohen I, Eyal-Shaham L, Ben-Zvi O, Tikochinski Y, Loya Y. 2019. Photoacclimation and induction of light-enhanced calcification in the mesophotic coral *Euphyllia paradivisa*. *Royal Society Open Science* **6**. doi:10.1098/rsos.180527

Eyal G, Wiedenmann J, Grinblat M, D'Angelo C, Kramarsky-Winter E, Treibitz T, Ben-Zvi O, Shaked Y, Smith TB, Harii S, Denis V, Noyes T, Tamir R, Loya Y. 2015. Spectral diversity and regulation of coral fluorescence in a mesophotic reef habitat in the Red Sea. *PLoS ONE* **10**:e0128697. doi:10.1371/journal.pone.0128697

Falkowski PG, Dubinsky Z. 1981. Light-shade adaptation of *Stylophora pistillata*, a hermatypic coral from the Gulf of Eilat. *Nature* **289**:172–174. doi:10.1038/289172a0

Field S, Bulina M, Kelmanson I, Bielawski J, Matz M. 2006. Adaptive evolution of multicolored fluorescent proteins in reef-building corals. *Journal of Molecular Evolution* **62**:332–339. doi:10.1007/s00239-005-0129-9

Fisher R, O'Leary RA, Low-Choy S, Mengersen K, Knowlton N, Brainard RE, Caley MJ. 2015. Species richness on coral reefs and the pursuit of convergent global estimates. *Current Biology* **25**:500–505. doi:10.1016/j.cub.2014.12.022

Gittins JR, D'Angelo C, Oswald F, Edwards RJ, Wiedenmann J. 2015. Fluorescent protein-mediated colour polymorphism in reef corals: multicopy genes extend the

adaptation/acclimatization potential to variable light environments. *Mol Ecol* **24**:453–465. doi:10.1111/mec.13041

Gorbunov MY, Kolber ZS, Lesser MP, Falkowski PG. 2001. Photosynthesis and photoprotection in symbiotic corals. *Limnology and Oceanography* **46**:75–85. doi:10.4319/lo.2001.46.1.0075

Grégoire V, Schmacka F, Coffroth MA, Karsten U. 2017. Photophysiological and thermal tolerance of various genotypes of the coral endosymbiont <i>Symbiodinium<i/> sp. (Dinophyceae). *Journal of Applied Phycology* **29**:1893–1905. doi:10.1007/s10811-017-1127-1

Harland AD, Spencer Davies P, Fixter LM. 1992. Lipid content of some Caribbean corals in relation to depth and light. *Marine Biology* **113**:357–361. doi:10.1007/BF00349159

Helmuth BST, Timmerman BEH, Sebens KP. 1997. Interplay of host morphology and symbiont microhabitat in coral aggregations. *Marine Biology* **130**:1–10. doi:10.1007/s002270050219

Hennige S, Smith D, Perkins R, Consalvey M, Paterson D, Suggett D. 2008. Photoacclimation, growth and distribution of massive coral species in clear and turbid waters. *Marine Ecology Progress Series* **369**:77–88. doi:10.3354/meps07612

Hoegh-Guldberg O, Jones RJ. 1999. Photoinhibition and photoprotection in symbiotic dinoflagellates from reef-building corals. *Marine Ecology Progress Series* **183**:73–86. doi:10.3354/meps183073

Hoogenboom MO, Connolly SR, Anthony KRN. 2008. Interactions between morphological and physiological plasticity optimize energy acquisition in corals. *Ecology* **89**:1144–1154. doi:10.1890/07-1272.1

Id HY, Koike K, Shinzato C, Jimbo M, Suzuki G. 2021. Can *Acropora tenuis* larvae attract native Symbiodiniaceae cells by green fluorescence at the initial establishment of symbiosis? *PLoS One* **16**:e0252514. doi:10.1371/journal.pone.0252514

Jacques SL. 2013. Optical properties of biological tissues: a review. *Physics in Medicine and Biology* **58**:R37–R61. doi:10.1088/0031-9155/58/11/r37

Jiang J, Zhang H, Kang Y, Bina D, Lo CS, Blankenship RE. 2012. Characterization of the peridinin-chlorophyll a-protein complex in the dinoflagellate *Symbiodinium*. *Biochimica et Biophysica Acta - Bioenergetics* **1817**:983–989. doi:10.1016/j.bbabio.2012.03.027

Jimenez IM, Larkum AWD, Ralph PJ, Kühl M. 2012. *In situ* thermal dynamics of shallow water corals is affected by tidal patterns and irradiance. *Marine Biology* **159**:1773–1782. doi:10.1007/s00227-012-1968-8

Jones R, Giofre N, Luter HM, Neoh TL, Fisher R, Duckworth A. 2020. Responses of corals to chronic turbidity. *Scientific Reports* **10**:1–13. doi:10.1038/s41598-020-61712-w

Kahng SE, Akkaynak D, Shlesinger T, Hochberg EJ, Wiedenmann J, Tamir R, Tchernov D. 2019. Light, temperature, photosynthesis, heterotrophy, and the lower depth limits of mesophotic coral ecosystems In: Loya Y, Puglise KA, Bridge TCL, editors. Mesophotic Coral Ecosystems. Cham: Springer International Publishing. pp. 801–828. doi:10.1007/978-3-319-92735-0_42

Kahng SE, Hochberg EJ, Apprill A, Wagner D, Luck DG, Perez D, Bidigare RR. 2012. Efficient light harvesting in deep-water zooxanthellate corals. *Marine Ecology Progress Series* **455**:65–77. doi:10.3354/meps09657

Kahng SE, Kelley CD. 2007. Vertical zonation of megabenthic taxa on a deep photosynthetic reef (50-140 m) in the Au'au Channel, Hawaii. *Coral Reefs* **26**:679–687. doi:10.1007/s00338-007-0253-7

Kahng SE, Watanabe TK, Hu HM, Watanabe T, Shen CC. 2020. Moderate zooxanthellate coral growth rates in the lower photic zone. *Coral Reefs* **39**:1273–1284. doi:10.1007/s00338-020-01960-4

Kaniewska P, Anthony KRN, Sampayo EM, Campbell PR, Hoegh-Guldberg O. 2014. Implications of geometric plasticity for maximizing photosynthesis in branching corals. *Marine Biology* **161**:313–328. doi:10.1007/s00227-013-2336-z

Kaniewska P, Magnusson SH, Anthony KRN, Reef R, Kühl M, Hoegh-Guldberg O. 2011. Importance of macro- versus microstructure in modulating light levels inside coral colonies. *Journal of Phycology* **47**:846–860. doi:10.1111/j.1529-8817.2011.01021.x

Kaniewska P, Sampayo EM. 2022. Macro- and micro-scale adaptations allow distinct *Stylophora pistillata*-symbiodiniaceae holobionts to optimize performance across a broad light habitat. *Journal of Phycology* **58**:55–70. doi:10.1111/jpy.13215

Kirk JTO. 1994. Light and photosynthesis in aquatic ecosystems. Cambridge University Press. doi:10.1017/CBO9780511623370

Kleypas JA, McManu JW, Mene LAB. 1999. Environmental limits to coral reef development: Where do we draw the line? *American Zoologist* **39**:146–159. doi:10.1093/icb/39.1.146

Kramer N, Guan J, Chen S, Wangpraseurt D, Loya Y. 2021. Characterization of morpho-functional traits in mesophotic corals reveals optimized light capture and photosynthesis. *bioRxiv*. doi:10.1101/2021.09.29.462347

Kramer N, Tamir R, Ben-Zvi O, Jacques SL, Loya Y, Wangpraseurt D. 2020. Light-harvesting in mesophotic corals is powered by a spatially efficient photosymbiotic system between coral host and microalgae. *bioRxiv*. doi:10.1101/2020.12.04.411496

Kühl M. 2005. Optical microsensors for analysis of microbial communities In: Leadbetter JR, editor. Environmental Microbiology. Academic Press. pp. 166–199. doi:10.1016/S0076-6879(05)97010-9

Kühl M, Cohen Y, Dalsgaard T, Jorgensen BB, Revsbech NP. 1995. Microenvironment and photosynthesis of zooxanthellae in scleractinian corals studied with microsensors for 0_2, pH and light. *Marine Ecology Progress Series* **117**:159-172.1995. doi:10.3354/meps117159

Leinbach SE, Speare KE, Rossin AM, Holstein DM, Strader ME. 2021. Energetic and reproductive costs of coral recovery in divergent bleaching responses. *Scientific Reports* 1–10. doi:10.1038/s41598-021-02807-w

Lesser MP, Slattery M, Leichter JJ. 2009. Ecology of mesophotic coral reefs. *Journal of Experimental Marine Biology and Ecology* **375**:1–8. doi:10.1016/j.jembe.2009.05.009

Lesser MP, Slattery M, Stat M, Ojimi M, Gates RD, Grottoli A. 2010. Photoacclimatization by the coral *Montastraea cavernosa* in the mesophotic zone: light, food, and genetics. *Ecology* **91**:990–1003. doi:10.1890/09-0313.1

Leutenegger A, D'Angelo C, Matz M V, Denzel A, Oswald F, Salih A, Nienhaus GU, Wiedenmann J. 2007. It's cheap to be colorful. *FEBS Journal* **274**:2496–2505. doi:10.1111/j.1742-4658.2007.05785.x

Levy O, Dubinsky Z, Achituv Y. 2003. Photobehavior of stony corals: responses to light spectra and intensity. *Journal of Experimental Biology* **206**:4041–4049. doi:10.1242/jeb.00622

Lichtenberg M, Brodersen KE, Kühl M. 2017. Radiative energy budgets of phototrophic surface-associated microbial communities and their photosynthetic efficiency under diffuse and collimated light. *Frontiers in Microbiology* **8**:1–17. doi:10.3389/fmicb.2017.00452

Lichtenberg M, Larkum AWD, Kühl M. 2016. Photosynthetic acclimation of *Symbiodinium* in hospite depends on vertical position in the tissue of the scleractinian coral *Montastrea curta*. *Frontiers in Microbiology* **7**. doi:10.3389/fmicb.2016.00230

Lohr KE, Camp EF, Kuzhiumparambil U, Lutz A, Leggat W, Patterson JT, Suggett DJ. 2019. Resolving coral photoacclimation dynamics through coupled photophysiological and metabolomic profiling. *Journal of Experimental Biology* **222**. doi:10.1242/jeb.195982

López-Londoño T, Galindo-Martínez CT, Gómez-Campo K, González-Guerrero LA, Roitman S, Pollock FJ, Pizarro V, López-Victoria M, Medina M, Iglesias-Prieto R. 2021. Physiological and ecological consequences of the water optical properties degradation on reef corals. *Coral Reefs* **40**:1243–1256. doi:10.1007/s00338-021-02133-7

Lough JM, Barnes DJ. 2000. Environmental controls on growth of the massive coral *Porites*. *Journal of Experimental Marine Biology and Ecology* **245**:225–243. doi:10.1016/s0022-0981(99)00168-9

Lyndby NH, Holm JB, Wangpraseurt D, Ferrier-Pagès C, Kühl M. 2019. Bio-optical properties and radiative energy budgets in fed and unfed scleractinian corals (*Pocillopora* sp.) during thermal bleaching. *Marine Ecology Progress Series* **629**:1–17. doi:10.3354/meps13146

Lyndby NH, Kuhl M, Wangpraseurt D. 2016. Heat generation and light scattering of green fluorescent protein-like pigments in coral tissue. *Scientific Reports* **6**:26599. doi:10.1038/srep26599

Marcelino LA, Westneat MW, Stoyneva V, Henss J, Rogers JD, Radosevich A, Turzhitsky V, Siple M, Fang A, Swain TD, Fung J, Backman V. 2013. Modulation of light-enhancement to symbiotic algae by light-scattering in corals and evolutionary trends in bleaching. *PLoS ONE* **8**:e61492. doi:10.1371/journal.pone.0061492

Martinez S, Kolodny Y, Shemesh E, Scucchia F, Nevo R, Levin-Zaidman S, Paltiel Y, Keren N, Tchernov D, Mass T. 2020. Energy sources of the depth-generalist mixotrophic coral *Stylophora pistillata*. *Front Mar Sci* **7**. doi:10.3389/fmars.2020.566663

Matz M v, Fradkov AF, Labas YA, Savitsky AP, Zaraisky AG, Markelov ML, Lukyanov SA. 1999. Fluorescent proteins from nonbioluminescent Anthozoa species. *Nature Biotechnology* **17**:969–973. doi:10.1038/13657

Muko S, Kawasaki K, Sakai K, Takasu F, Shigesada N. 2000. Morphological plasticity in the coral *Porites sillimaniani* and its adaptive significance. *Bulletin of Marine Science* **66**:225–239.

Muscatine L. 1990. The role of symbiotic algae in carbon and energy flux in coral reefs In: Dubinsky Z, editor. Ecosystems of the World, 25. Coral Reefs. Amsterdam: Elsevier. pp. 75–87.

Nienhaus GU, Wiedenmann J. 2009. Structure, dynamics and optical properties of fluorescent proteins: perspectives for marker development. *ChemPhysChem* **10**:1369–1379. doi:10.1002/cphc.200800839

Nir O, Gruber DF, Einbinder S, Kark S, Tchernov D. 2011. Changes in scleractinian coral *Seriatopora hystrix* morphology and its endocellular *Symbiodinium* characteristics along a bathymetric gradient from shallow to mesophotic reef. *Coral Reefs* **30**:1089–1100. doi:10.1007/s00338-011-0801-z

Oswald F, Schmitt F, Leutenegger A, Ivanchenko S, D'Angelo C, Salih A, Maslakova S, Bulina M, Schirmbeck R, Nienhaus GU, Matz M v, Wiedenmann J. 2007. Contributions of host and symbiont pigments to the coloration of reef corals. *FEBS Journal* **274**:1102–1122. doi:10.1111/j.1742-4658.2007.05661.x

Parkins SKT, Murthy S, Picioreanu C, Kühl M. 2021. Multiphysics modelling of photon, mass and heat transfer in coral microenvironments. *Journal of the Royal Society Interface* **18**:20210532. doi:10.1098/rsif.2021.0532

Quick C, D'Angelo C, Wiedenmann J. 2018. Trade-offs associated with photoprotective Green Fluorescent Protein expression as potential drivers of balancing selection for color polymorphism in reef corals. *Front Mar Sci* **5**:1–11. doi:10.3389/fmars.2018.00011

Ralph PJ, Gademann R, Larkum AWD, Kühl M. 2002. Spatial heterogeneity in active chlorophyll fluorescence and PSII activity of coral tissues. *Marine Biology* **141**:639–646. doi:10.1007/s00227-002-0866-x

Rickelt LF, Lichtenberg M, Trampe ECL, Kühl M. 2016. Fiber-optic probes for small-scale measurements of scalar irradiance. *Photochemistry and Photobiology* **92**:331–342. doi:10.1111/php.12560

Rocker MM, Francis DS, Fabricius KE, Willis BL, Bay LK. 2019. Temporal and spatial variation in fatty acid composition in *Acropora tenuis* corals along water quality gradients on the Great Barrier Reef, Australia. *Coral Reefs* **38**:215–228. doi:10.1007/s00338-019-01768-x

Rosset S, Wiedenmann J, Reed AJ, D'Angelo C. 2017. Phosphate deficiency promotes coral bleaching and is reflected by the ultrastructure of symbiotic dinoflagellates. *Marine Pollution Bulletin* **118**:180–187. doi:10.1016/J.MARPOLBUL.2017.02.044

Rouzé H, Galand PE, Medina M, Bongaerts P, Pichon M, Pérez-Rosales G, Torda G, Moya A, Bardout G, Périé-Bardout E, Marivint E, Lagarrigue G, Leblond J, Gazzola F, Pujolle

S, Mollon N, Mittau A, Fauchet J, Paulme N, Pete R, Peyrusse K, Ferucci A, Magnan A, Horlaville M, Breton C, Gouin M, Markocic T, Jubert I, Herrmann P, Raina JB, Hédouin L. 2021. Symbiotic associations of the deepest recorded photosynthetic scleractinian coral (172 m depth). *ISME Journal* **15**:1564–1568. doi:10.1038/s41396-020-00857-y

Salih A, Larkum A, Cox G, Kühl M, Hoegh-Guldberg O. 2000. Fluorescent pigments in corals are photoprotective. *Nature* **408**:850–853. doi:10.1038/35048564

Scheufen T, Iglesias-Prieto R, Enríquez S. 2017. Changes in the number of symbionts and *Symbiodinium* cell pigmentation modulate differentially coral light absorption and photosynthetic performance. *Front Mar Sci* **4**:1–17. doi:10.3389/fmars.2017.00309

Schlichter D, Meier U, Fricke HW. 1994. Improvement of photosynthesis in zooxanthellate corals by autofluorescent chromatophores. *Oecologia* **99**:124–131. doi:10.1007/BF00317092

Shagin DA, Barsova E V, Yanushevich YG, Fradkov AF, Lukyanov KA, Labas YA, Semenova TN, Ugalde JA, Meyers A, Nunez JM, Widder EA, Lukyanov SA, Matz M V. 2004. GFP-like proteins as ubiquitous metazoan superfamily: evolution of functional features and structural complexity. *Molecular Biology and Evolution* **21**:841–850. doi:10.1093/molbev/msh079

Shimomura O, Johnson FH, Saiga Y. 1962. Extraction, purification and properties of aequorin, a bioluminescent protein from the luminous hydromedusan, *Aequorea*. *J Cell Comp Physiol* **59**:223–239.

Smith EG, D'Angelo C, Salih A, Wiedenmann J. 2013. Screening by coral green fluorescent protein (GFP)-like chromoproteins supports a role in photoprotection of zooxanthellae. *Coral Reefs* **32**:463–474. doi:10.1007/s00338-012-0994-9

Smith EG, D'Angelo C, Sharon Y, Tchernov D, Wiedenmann J. 2017. Acclimatization of symbiotic corals to mesophotic light environments through wavelength transformation by fluorescent protein pigments. *Proceedings of the Royal Society of London B: Biological Sciences* **284**.

Soto D, de Palmas S, Ho MJ, Denis V, Chen CA. 2019. Spatial variation in the morphological traits of *Pocillopora verrucosa* along a depth gradient in Taiwan. *PLoS ONE* **13**. doi:10.1371/journal.pone.0202586

Szabó M, Wangpraseurt D, Tamburic B, Larkum AWD, Schreiber U, Suggett DJ, Kühl M, Ralph PJ. 2014. Effective light absorption and absolute electron transport rates in the coral *Pocillopora damicornis*. *Plant Physiology and Biochemistry* **83**:159–167. doi:10.1016/j.plaphy.2014.07.015

Tamir R, Ben-Zvi O, Eyal G, Kramer N, Loya Y. 2020. Reciprocal-transplantation between shallow and mesophotic stony corals. *Marine Environmental Research* **161**. doi:10.1016/j.marenvres.2020.105035

Tamir R, Eyal G, Kramer N, Laverick JH, Loya Y. 2019. Light environment drives the shallow-to-mesophotic coral community transition. *Ecosphere* **10**. doi:10.1002/ecs2.2839

Titlyanov EA, Titlyanova T v, Yamazato K, van Woesik R. 2001. Photo-acclimation dynamics of the coral *Stylophora pistillata* to low and extremely low light. *Journal of Experimental Marine Biology and Ecology* **263**:211–225. doi:10.1016/S0022-0981(01)00309-4

Todd PA. 2008. Morphological plasticity in scleractinian corals. *Biological Reviews* **83**:315–337. doi:10.1111/j.1469-185X.2008.00045.x

Ugalde JA, Chang BSW, Matz M. 2004. Evolution of coral pigments recreated. *Science (1979)* **305**:1433. doi:10.1126/science.1099597

Veal CJ, Carmi M, Dishon G, Sharon Y, Michael K, Tchernov D, Hoegh-Guldberg O, Fine M. 2010. Shallow-water wave lensing in coral reefs: a physical and biological case study. *The Journal of Experimental Biology* **213**:4304–4312. doi:10.1242/jeb.044941

Vogelmann TC, Evans JR. 2002. Profiles of light absorption and chlorophyll within spinach leaves from chlorophyll fluorescence. *Plant, Cell and Environment* **25**:1313–1323. doi:10.1046/j.1365-3040.2002.00910.x

Wangpraseurt D, Holm JB, Larkum AWD, Pernice M, Ralph PJ, Suggett DJ, Kühl M. 2017a. *In vivo* microscale measurements of light and photosynthesis during coral bleaching:

Evidence for the optical feedback loop? *Frontiers in Microbiology* **8**:59. doi:10.3389/fmicb.2017.00059

Wangpraseurt D, Jacques S, Lyndby N, Holm JB, Pages CF, Kühl M. 2019. Microscale light management and inherent optical properties of intact corals studied with optical coherence tomography. *Journal of The Royal Society Interface* **16**:20180567. doi:10.1101/376723

Wangpraseurt D, Jacques SL, Petrie T, Kühl M. 2016a. Monte Carlo modeling of photon propagation reveals highly scattering coral tissue. *Frontiers in Plant Science* **7**:1404. doi:10.3389/fpls.2016.01404

Wangpraseurt D, Larkum AWD, Franklin J, Szabó M, Ralph PJ, Kühl M. 2014a. Lateral light transfer ensures efficient resource distribution in symbiont-bearing corals. *J Exp Biol* **217**:489–98. doi:10.1242/jeb.091116

Wangpraseurt D, Larkum AWD, Ralph PJ, Kühl M. 2012. Light gradients and optical microniches in coral tissues. *Front Microbiol* **3**:316. doi:10.3389/fmicb.2012.00316

Wangpraseurt D, Pernice M, Guagliardo P, Kilburn MR, Clode PL, Polerecky L, Kühl M. 2016b. Light microenvironment and single-cell gradients of carbon fixation in tissues of symbiont-bearing corals. *ISME Journal* **10**:788–792. doi:10.1038/ismej.2015.133

Wangpraseurt D, Polerecky L, Larkum AWD, Ralph PJ, Nielsen DA, Pernice M, Kühl M. 2014b. The *in situ* light microenvironment of corals. *Limnology and Oceanography* **59**:917–926. doi:10.4319/lo.2014.59.3.0917

Wangpraseurt D, Tamburic B, Szabó M, Suggett D, Ralph PJ, Kühl M. 2014c. Spectral effects on *Symbiodinium* photobiology studied with a programmable light engine. *PLoS ONE* **9**:e112809. doi:10.1371/journal.pone.0112809

Wangpraseurt D, Wentzel C, Jacques SL, Wagner M, Kühl M. 2017b. In vivo imaging of coral tissue and skeleton with optical coherence tomography. *Journal of the Royal Society Interface* **14**. doi:10.1098/rsif.2016.1003

Wangpraseurt D, You S, Azam F, Jacucci G, Gaidarenko O, Hildebrand M, Kühl M, Smith AG, Davey MP, Smith A, Deheyn DD, Chen S, Vignolini S. 2020. Bionic 3D printed corals. *Nature Communications* **11**. doi:10.1038/s41467-020-15486-4

Wiedenmann J, D'Angelo C, Smith EG, Hunt AN, Legiret F-E, Postle AD, Achterberg EP. 2013. Nutrient enrichment can increase the susceptibility of reef corals to bleaching. *Nature Climate Change* **3**:160–164. doi:10.1038/nclimate1661

Wiedenmann J, Ivanchenko S, Oswald F, Schmitt F, Röcker C, Salih A, Spindler K-D, Nienhaus GU. 2004. EosFP, a fluorescent marker protein with UV-inducible green-to-red fluorescence conversion. *Proc Natl Acad Sci U S A* **101**:15905–15910. doi:10.1073/pnas.0403668101

Wijgerde T, van Melis A, Silva CIF, Leal MC, Vogels L, Mutter C, Osinga R. 2014. Red light represses the photophysiology of the scleractinian coral *Stylophora pistillata*. *PLoS ONE* **9**:e92781. doi:10.1371/journal.pone.0092781

Willis BL. 1985. Phenotypic plasticity versus phenotypic stability in the reef corals *Turbinaria mesenterina* and *Pavona cactus*Proceedings of the Fifth International Coral Reef Symposium. pp. 107–112.

Winters G, Beer S, ben Zvi B, Brickner I, Loya Y. 2009. Spatial and temporal photoacclimation of stylophora pistillata: Zooxanthella size, pigmentation, location and clade. *Marine Ecology Progress Series* **384**:107–119. doi:10.3354/meps08036

986 **Figure legends**

987 **Figure 1. Spectral scalar irradiance in *M. cavernosa* under broad spectrum light. a**) $E_0(\lambda)$
988 at coenosarc surface, with excitation and emission peaks of unconverted and converted
989 pcRFP highlighted (colorful arrows), as well as absorption peaks of Symbiodiniaceae
990 photosynthetic pigments (black arrows). Mean (solid lines) + s.d. (dashed lines); n=3
991 measurements on 2 fragments. **b**) Spectral attenuation coefficient of $E_0(\lambda)$ from coenosarc
992 surface to skeleton (average thickness = 560 μm). Mean (solid lines) + s.d. (dashed line), n=3.
993

994 **Figure 2. Host pigment fluorescence distribution in the tissue of *M. cavernosa***
995 **undergoing photoconversion.** Scalar irradiance measurements collected under blue
996 excitation 455-505 nm (Figure 2—figure supplement 1 c). **a**) 514:582 nm emission ratio,
997 indicating the degree of photoconversion for each coral (*unconverted* >1, *partially converted*
998 ~1, *converted* <1). Boxplots show data for the surface and deepest data point, grouped as
999 *unconverted* vs *partially converted* or *converted*. Star represents adjusted p<0.05 in pairwise
1000 post-hoc comparison. **b**) Fluorescence micrographs of representative photoconversion
1001 stages. **c**) Normalised fluorescence emission profiles (arbitrary units, a.u.).
1002

1003 **Figure 3. Photon scalar irradiance of host pigment fluorescence in the tissue of *M.***
1004 ***cavernosa* at representative photoconversion stages. a**) Tissue surface emission
1005 spectra of *unconverted*, *partially converted* and *converted* specimens (ex = 455-505 nm). **b**)
1006 Integrated green (505-560 nm) and red (560-650 nm) fluorescence emission along a tissue
1007 depth profile, measured under blue excitation (455-505 nm, Figure 2—figure supplement 1
1008 c).
1009

1010 **Figure 4. Spectral photon irradiance and wavelength conversion in corals with photo-**
1011 **convertible host pigments along a depth gradient. a**) Integrated photon irradiance in the
1012 455-505 nm and 560-650 nm range measured on a mesophotic reef in Eilat, Red Sea (Eyal
1013 et al., 2015). **b**) Measured 560-650 nm light generated by pcRFP emission and estimated
1014 relative contribution to the total amount of 560-650 nm light available to the coral holobiont.
1015 Error bars represent range between measurement at the coral skeleton (1%) and
1016 measurement at the coral surface (5%).
1017

1018 **Figure 5. Effects of photoprotective chromoproteins on coral light environment. a**)
1019 Representative photographs of unbleached brown and bleached pink *P. damicornis*. **b**)
1020 Spectral scalar irradiance ($E_0(\lambda)$) measurements at the coenosarc surface of unbleached
1021 brown *P. damicornis*, bleached *P. damicornis* with high CP content, and *P. damicornis*
1022 skeleton. **c**) Spectral attenuation coefficient ($K_0(\lambda)$) of scalar irradiance for unbleached brown
1023 and bleached pink *P. damicornis*, calculated from surface to skeleton (tissue thickness =
1024 ~300 μm). **d**) Compilation of representative photographs of the unbleached high CP morph,
1025 unbleached no CP morph and bleached no CP morph of *M. foliosa*. **e**) Surface $E_0(\lambda)$
1026 measurements of unbleached inner region (low CP), unbleached margin (high CP) and
1027 bleached no CP morph of *M. foliosa*. In **a** and **d**, scale bar = 5 mm. In **b** and **e**, mean (solid
1028 lines) + s.d. (dashed lines), n=3 measurements. Arrows indicate peak absorption wavelength
1029 in nm for symbiont photosynthetic pigments (black) and CPs (pink).
1030 **Figure supplement legends**
1031

Figure 2—figure supplement 1. The scalar irradiance measurement set up (**a**) and spectra of the two light sources used for measurement (KL-1600 LED, **b**; xenon arc lamp + GFPplus filter, **c**). In **c**, dashed lines represent field measurements from 80 m depth in the Red Sea (Eyal et al. 2015), normalized to integrated irradiance.

Figure 2—figure supplement 2. Spectra of light sources used for photoconversion (**a**-**c**) and bleaching (**d**,**e**) experiments (**a**, Lumiled Luxeon Rebel Green; **b**, xenon arc lamp + UV bandpass; **c**, Aquaray NUV; **d**, Lumiled Luxeon Rebel Deep Red; **e**, Lumiled Luxeon Rebel Royal Blue)

Figure 3—figure supplement 1. Photon scalar irradiance in the tissue of green and red morphs of *Echinophyllia*. **a**) Fluorescence micrographs (**a**) and surface fluorescence emission (**b**) of green and red morphs. **c**) Integrated green (505-560 nm) and red (560-650 nm) fluorescence emission along a tissue depth profile, measured under blue excitation (455-505 nm, Fig. S1). Spheres show means ± s.d., n=3.

Figure 4—figure supplement 1. Relative contribution of fluorescence emission by pcRFPs and downwelling irradiance to the total 560-650 nm light available to pcRFP-containing corals along a depth gradient in the Bahamas (modelled irradiance data from Lesser et al. 2009).

Appendix 1

Incident intensity calibration (Supplementary Methods)

To determine whether the relationship between excitation light intensity and emitted fluorescence was linear within our measurement range, we performed a calibration profile on a *converted M. cavernosa* sample using a set of neutral density filters. At each depth, we collected fluorescence emission measurements under 455-505 nm excitation with five combinations of neutral density filters placed between the excitation light and the specimen. We then calculated the integrated photon scalar irradiance in the incident range (455-505 nm) at each tissue depth, the integrated green fluorescence emission (505-560 nm, Appendix 1—figure 1a) and the integrated red fluorescence emission (560-610 nm, Appendix 1—figure 1b). A linear regression was fitted for each tissue depth and each chromophore, with intercept set to zero (Appendix 1—figure 1); p-values were corrected for multiple testing using the Bonferroni adjustment.

Appendix 1—table 1. Results of t-test with Bonferroni adjustment for Figure 1a.

Wavelength	t value	d. f.	P	Adjusted P
438	1.572583	3.165662	0.209155	1
476	1.49222	3.538786	0.218869	1
507	1.638856	3.678655	0.182766	1
514	1.754119	3.500689	0.164409	0.986453
571	1.946208	3.84537	0.126343	0.758061
670	1.553197	3.589537	0.203304	1

Appendix 1—table 2. Results of two-way ANOVA followed by Tukey test post-hoc comparison for Figure 2a

Factor	d. f.	Sum Sq	Mean Sq	F	P
Photoconversion	1	7.709	7.709	61.47	<0.001
Tissue depth	1	1.646	1.646	13.13	0.007
Photoconv:depth	1	2.301	2.301	18.35	0.003
Residuals	8	1.003	0.125		

	Diff	Lower	Upper	Adjusted P
Photoconversion				
Unconv vs Conv	1.603	1.132	2.075	<0.001
Tissue depth				
Surface vs Deep	0.741	0.269	1.212	0.007
Photoconv:depth				
Unconv.Deep vs Conv.Deep	0.727	-0.199	1.653	0.132
Conv.Surface vs Conv.Deep	-0.135	-1.061	0.791	0.964
Unconv.Surface vs Conv.Deep	2.344	1.418	3.270	<0.001
Conv.Surface vs Unconv.Deep	-0.862	-1.788	0.064	0.068
Unconv.Surface vs Unconv.Deep	1.617	0.691	2.543	0.002
Unconv.Surf vs Conv.Surf	2.478	1.553	3.405	<0.001

Appendix 1—table 3. Results of linear regression with Bonferroni adjustment for multiple testing for Appendix 1—figure 1.

Green (505-560 nm) fluorescence emission

Depth	Slope	Std Error	t value	R^2 adjusted	P	Adjusted P
0	0.00902626	9.03E-05	99.9875929	0.99950008	6.00E-08	6.00E-07
70	0.0087601	7.62E-05	114.967832	0.99962183	3.43E-08	3.43E-07
140	0.01156811	0.00021343	54.2017461	0.99830038	6.94E-07	6.94E-06
210	0.01619148	0.00017715	91.4024378	0.9994018	8.59E-08	8.59E-07
280	0.02494033	0.00019703	126.581943	0.99968803	2.34E-08	2.34E-07
350	0.03021069	0.00018083	167.069327	0.99982089	7.70E-09	7.70E-08
420	0.03351092	0.0003004	111.554686	0.99959834	3.87E-08	3.87E-07
490	0.033718	0.00022538	149.603347	0.99977664	1.20E-08	1.20E-07
560	0.02842214	0.00042339	67.1300277	0.99889146	2.95E-07	2.95E-06
630	0.01999956	0.00028305	70.6577889	0.9989993	2.40E-07	2.40E-06

Red (560-650 nm) fluorescence emission

Depth	Slope	Std Error	t value	R^2 adjusted	P	Adjusted P
0	0.01719483	8.20E-05	209.593244	0.99988619	3.11E-09	3.11E-08
70	0.01510699	6.92E-05	218.286085	0.99989507	2.64E-09	2.64E-08
140	0.01881416	0.00019939	94.3604722	0.9994387	7.56E-08	7.56E-07
210	0.0266481	8.29E-05	321.256566	0.99995155	5.63E-10	5.63E-09
280	0.04096949	0.00025024	163.718467	0.99981349	8.35E-09	8.35E-08
350	0.05367283	0.00046253	116.040816	0.99962879	3.31E-08	3.31E-07
420	0.07300642	0.00047553	153.525421	0.9997879	1.08E-08	1.08E-07
490	0.09251997	0.00093074	99.4042684	0.99949419	6.14E-08	6.14E-07
560	0.08291338	0.00118633	69.8904363	0.99897723	2.51E-07	2.51E-06
630	0.06235948	0.00053652	116.22921	0.99962999	3.29E-08	3.29E-07

Appendix 1—table 4. List of acclimation conditions, experimental treatments and measurements performed on each species and morph used in the study.

Species and morph	Acclimation	Experimental treatment	Measurements
M. cavernosa	40 days green light	None	E_0 profiles (white illumination)
		Exposure to xenon arc lamp +UV filter for 6 hours localised to a 3 mm spot	E_0 profiles inside and outside treated area (white and blue illumination)
		Exposure to NUV LED over the entire sample for 10 hours	E_0 profiles before and after treatment (white and blue illumination)
Echinophyllia sp. green morph	>6 months broad spectrum metal halide, 100 µmol photons m^{-2} s^{-1}	None	E_0 profiles (blue illumination)
Echinophyllia sp. red morph	>6 months broad spectrum metal halide, 100 µmol photons m^{-2} s^{-1}	None	E_0 profiles (blue illumination)
P. damicornis pink morph	>6 months broad spectrum metal halide, 100 µmol photons m^{-2} s^{-1}	Exposure to 400 µmol photons m^{-2} s^{-1} red light for 7 days followed by exposure to 100 µmol photons m^{-2} s^{-1} blue light for 20 days	E_0 profile and surface E_0 after treatment (white illumination)
P. damicornis brown morph	>6 months broad spectrum metal halide, 100 µmol photons m^{-2} s^{-1}	None	E_0 profile and surface E_0 after treatment (white illumination)
M. foliosa purple edge morph	>6 months broad spectrum metal halide, 200 µmol photons m^{-2} s^{-1}	None	Surface E_0 (white illumination)
M. foliosa brown morph	>6 months broad spectrum metal halide, 200 µmol photons m^{-2} s^{-1}	65 days high nitrate/low phosphate	Surface E_0 after treatment (white illumination)

Appendix 1 figure legends

Appendix 1—figure 1. Relationship between blue (455-505 nm) excitation light photon irradiance measured *in hospite* and emitted green (505-560 nm, **a**) or red (560-650 nm, **b**) fluorescence at 10 tissue depths, obtained with a set of neutral density filters. Trendlines represent fitted linear regression (adjusted $p<0.05$, table S1).

Figure 1

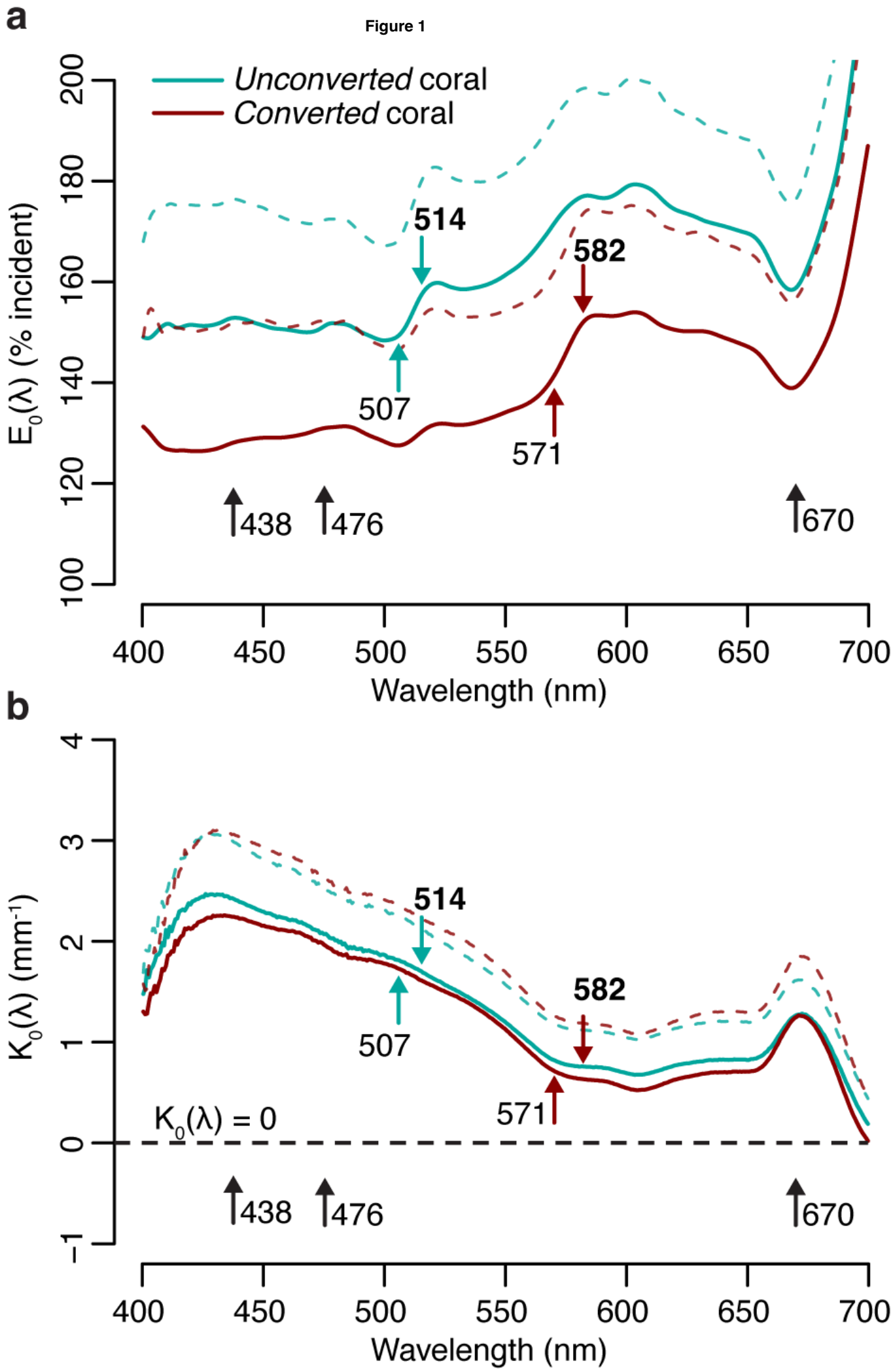
a
Unconverted coral
Converted coral
514
582
507
571
438
476
670
$E_0(\lambda)$ (% incident)
100
120
140
160
180
200
400
450
500
550
600
650
700
Wavelength (nm)
b
514
582
507
571
$K_0(\lambda) = 0$
438
476
670
$K_0(\lambda)$ (mm^{-1})
−1
0
1
2
3
4
400
450
500
550
600
650
700
Wavelength (nm)

Figure 2 - figure supplement 1

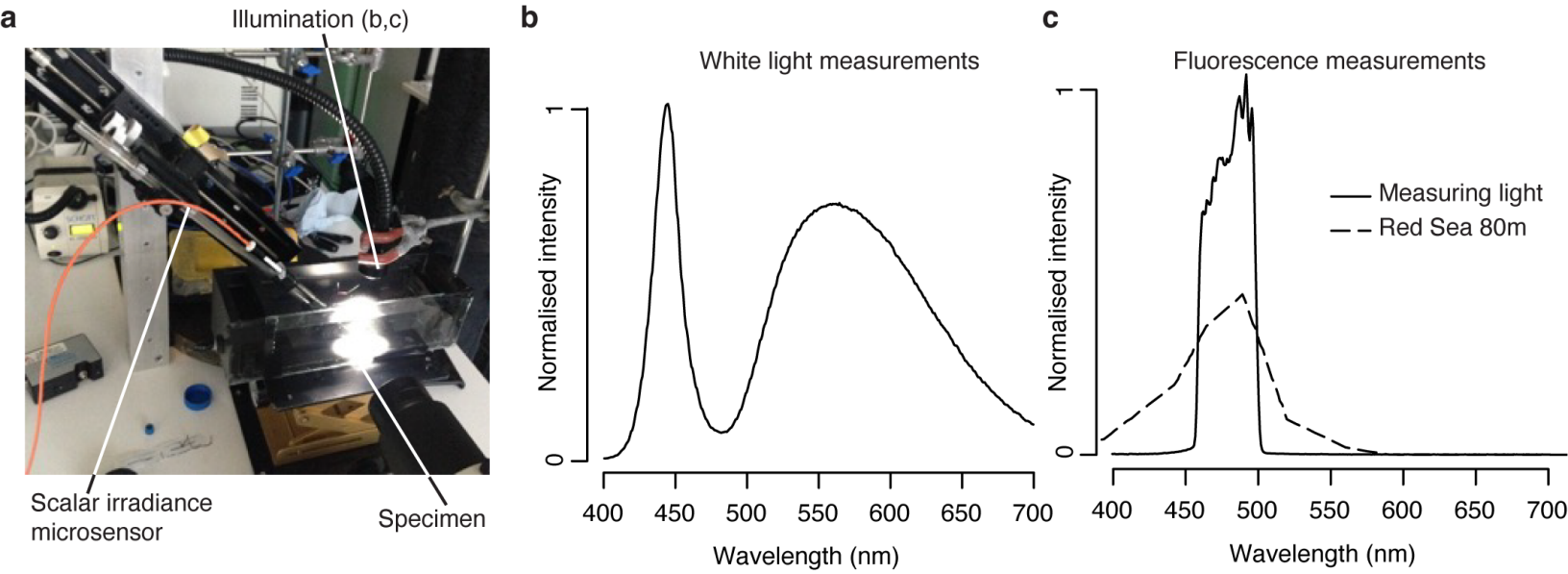

Figure 2 - figure supplement 2

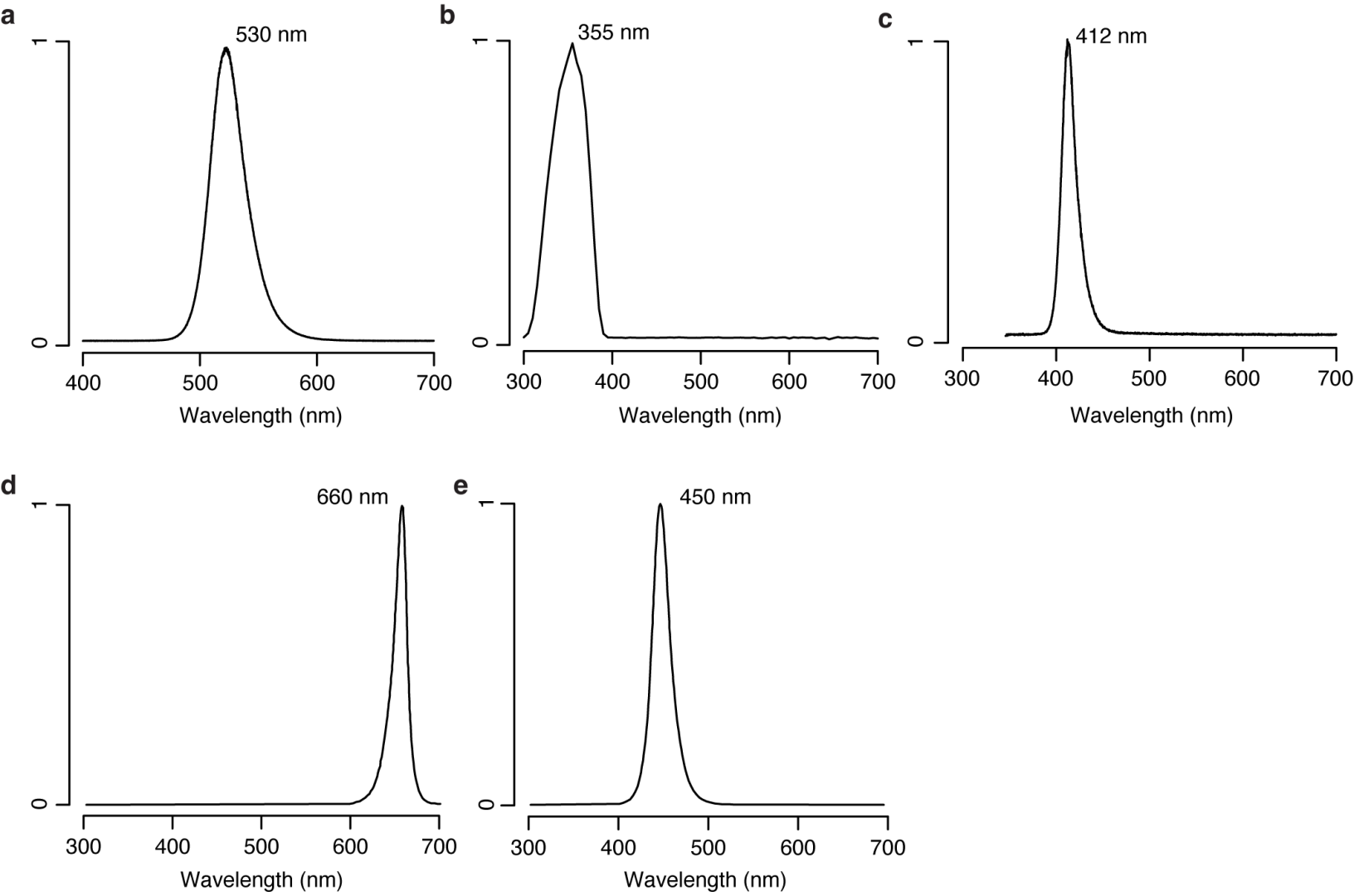

Figure 2

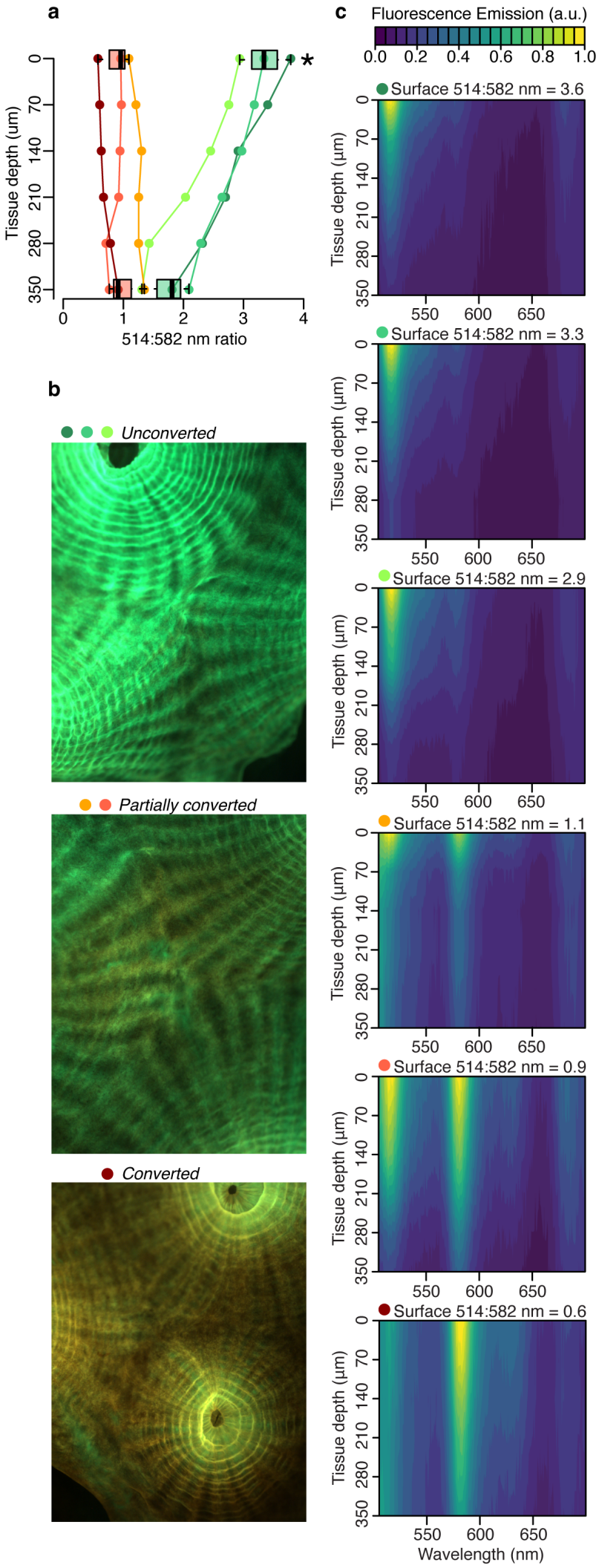
a
Tissue depth (um)
0
70
140
210
280
350
0
1
2
3
4
514:582 nm ratio
*
b
Unconverted
Partially converted
Converted
c
Fluorescence Emission (a.u.)
0.0
0.2
0.4
0.6
0.8
1.0
Surface 514:582 nm = 3.6
Surface 514:582 nm = 3.3
Surface 514:582 nm = 2.9
Surface 514:582 nm = 1.1
Surface 514:582 nm = 0.9
Surface 514:582 nm = 0.6
Tissue depth (µm)
550
600
650
Wavelength (nm)

Figure 3 - figure supplement 1

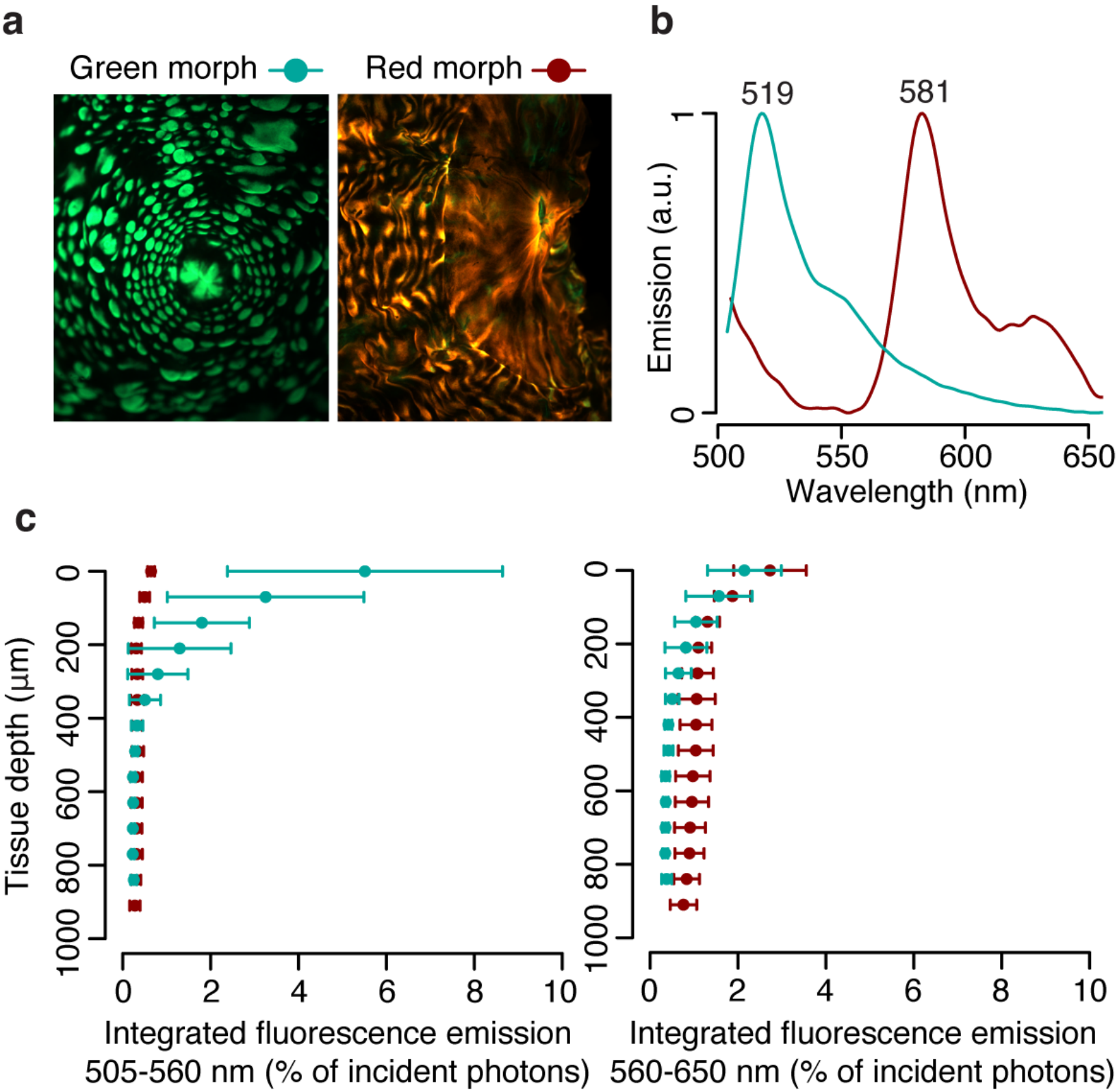

Figure 3

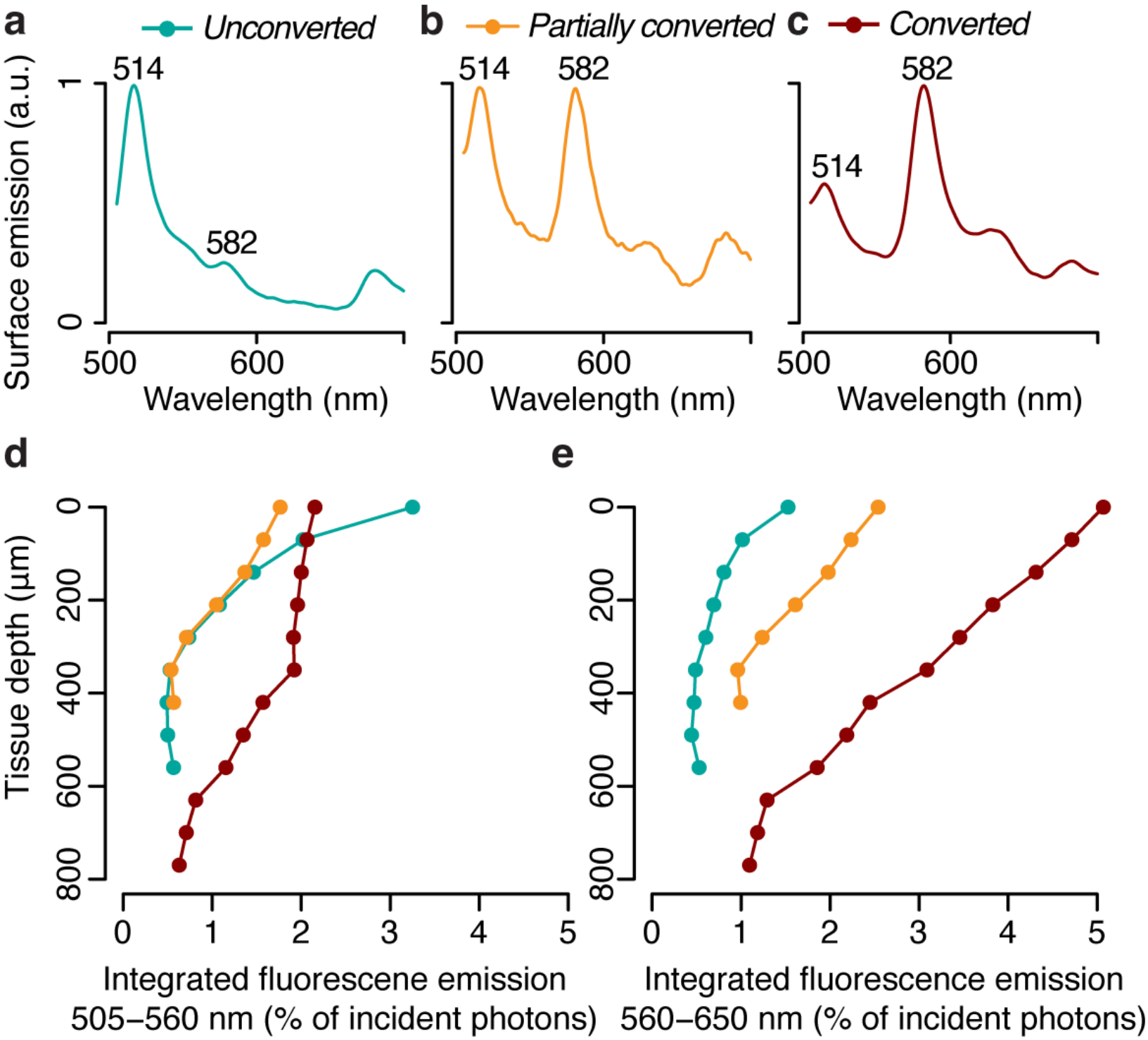
a
Unconverted
514
582
Surface emission (a.u.)
1
0
500
600
Wavelength (nm)
b
Partially converted
514
582
500
600
Wavelength (nm)
c
Converted
582
514
500
600
Wavelength (nm)
d
Tissue depth (µm)
0
200
400
600
800
0
1
2
3
4
5
Integrated fluorescene emission
505–560 nm (% of incident photons)
e
0
200
400
600
800
0
1
2
3
4
5
Integrated fluorescence emission
560–650 nm (% of incident photons)

Figure 4 - figure supplement 1

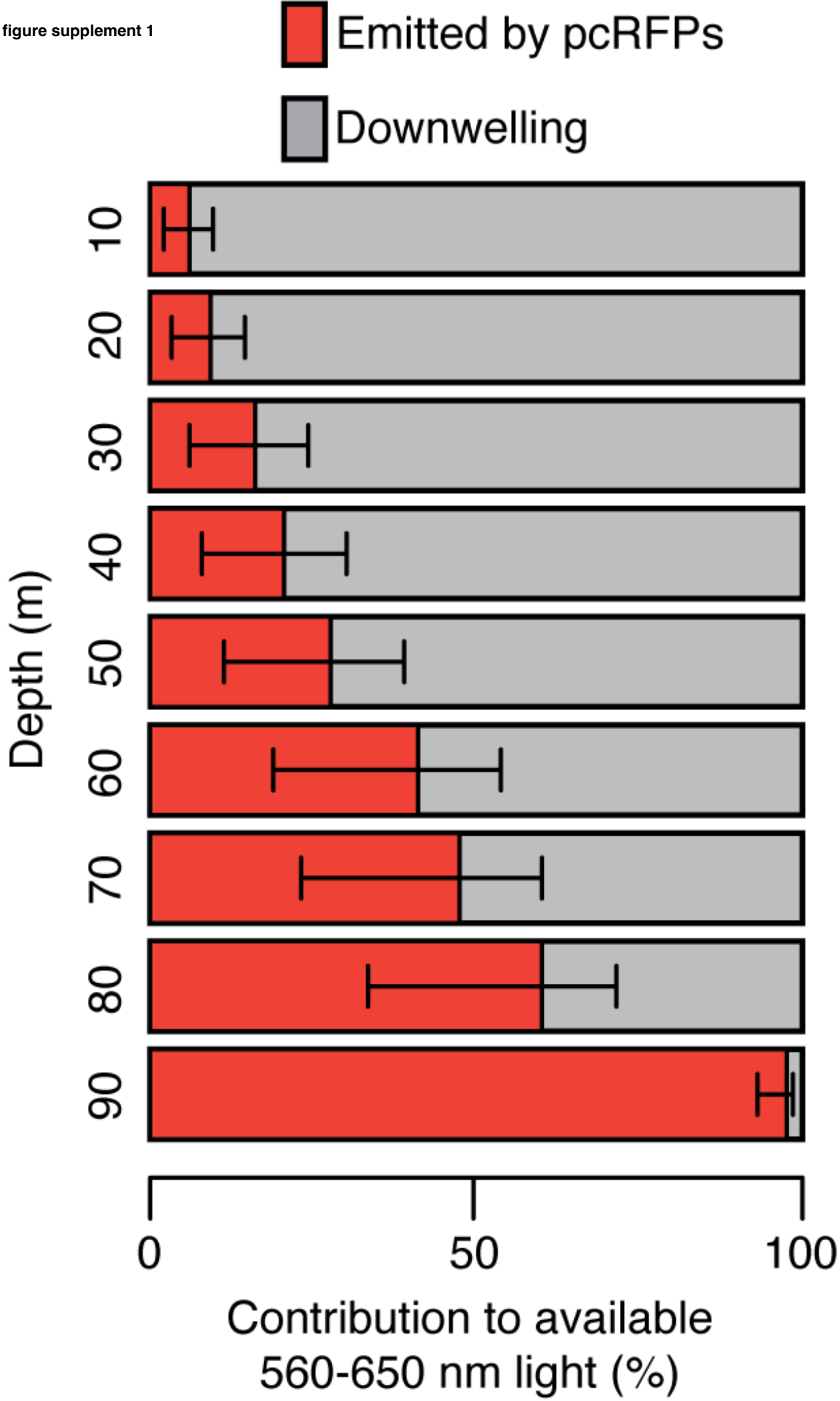

Figure 4

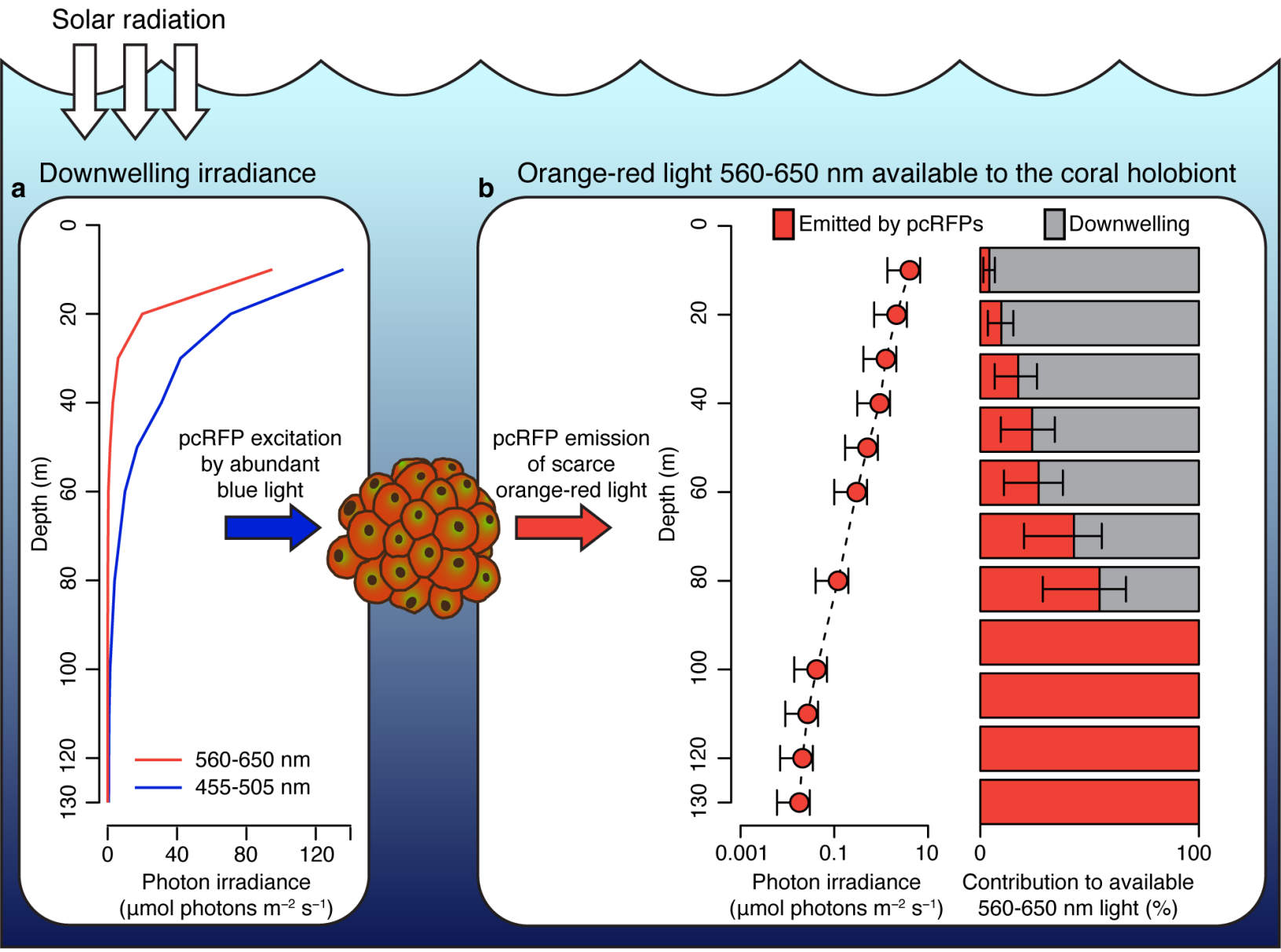
Solar radiation
a
Downwelling irradiance
Depth (m)
0
20
40
60
80
100
120
130
pcRFP excitation
by abundant
blue light
560-650 nm
455-505 nm
0
40
80
120
Photon irradiance
(µmol photons m⁻² s⁻¹)
b
Orange-red light 560-650 nm available to the coral holobiont
pcRFP emission
of scarce
orange-red light
Emitted by pcRFPs
Downwelling
0.001
0.1
10
0
100
Contribution to available
560-650 nm light (%)

Figure 5

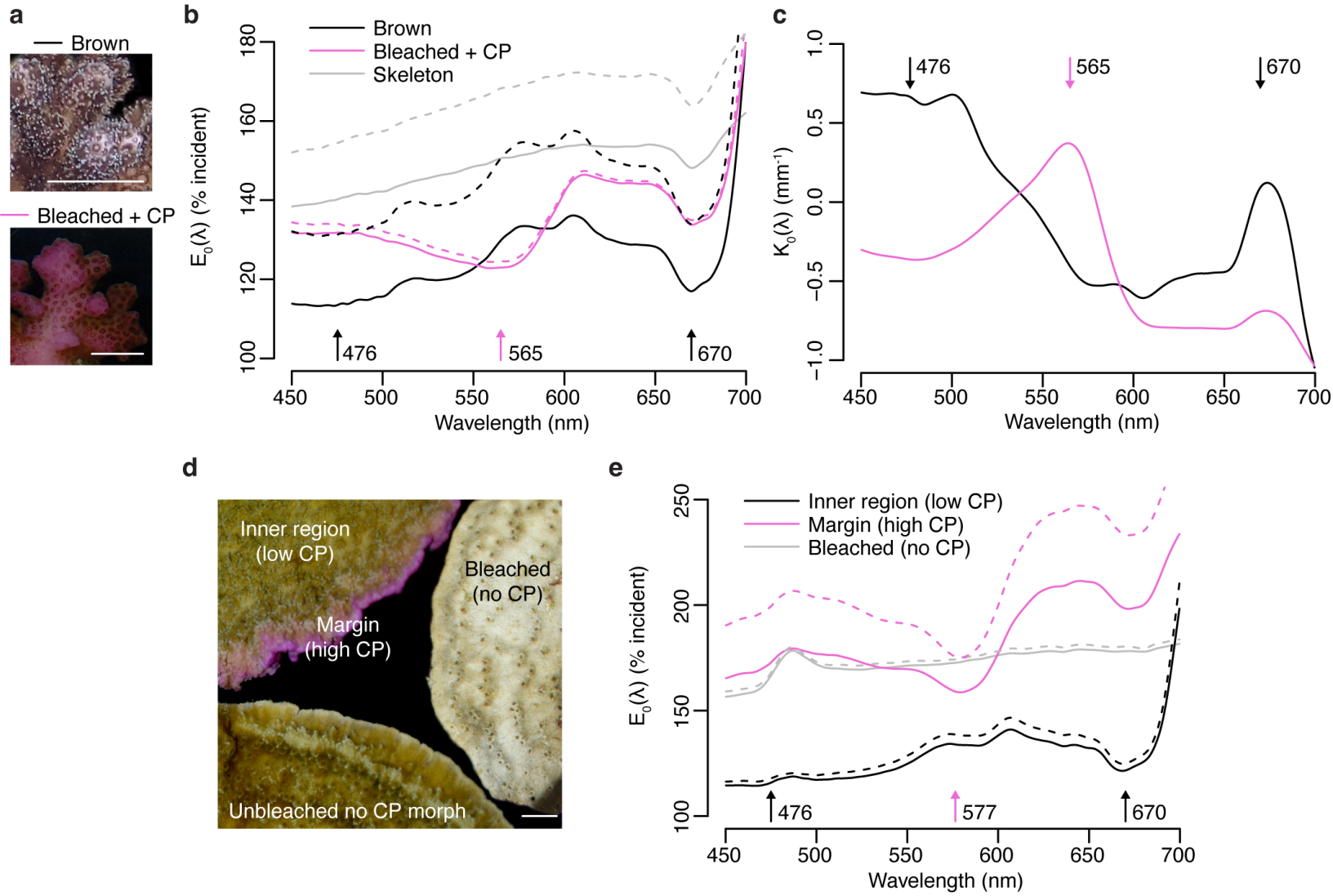
a
Brown
Bleached + CP
b
Brown
Bleached + CP
Skeleton
$E_0(\lambda)$ (% incident)
100
120
140
160
180
476
565
670
450
500
550
600
650
700
Wavelength (nm)
c
$K_0(\lambda)$ (mm^{-1})
−1.0
−0.5
0.0
0.5
1.0
476
565
670
450
500
550
600
650
700
Wavelength (nm)
d
Inner region
(low CP)
Margin
(high CP)
Bleached
(no CP)
Unbleached no CP morph
e
Inner region (low CP)
Margin (high CP)
Bleached (no CP)
$E_0(\lambda)$ (% incident)
100
150
200
250
476
577
670
450
500
550
600
650
700
Wavelength (nm)
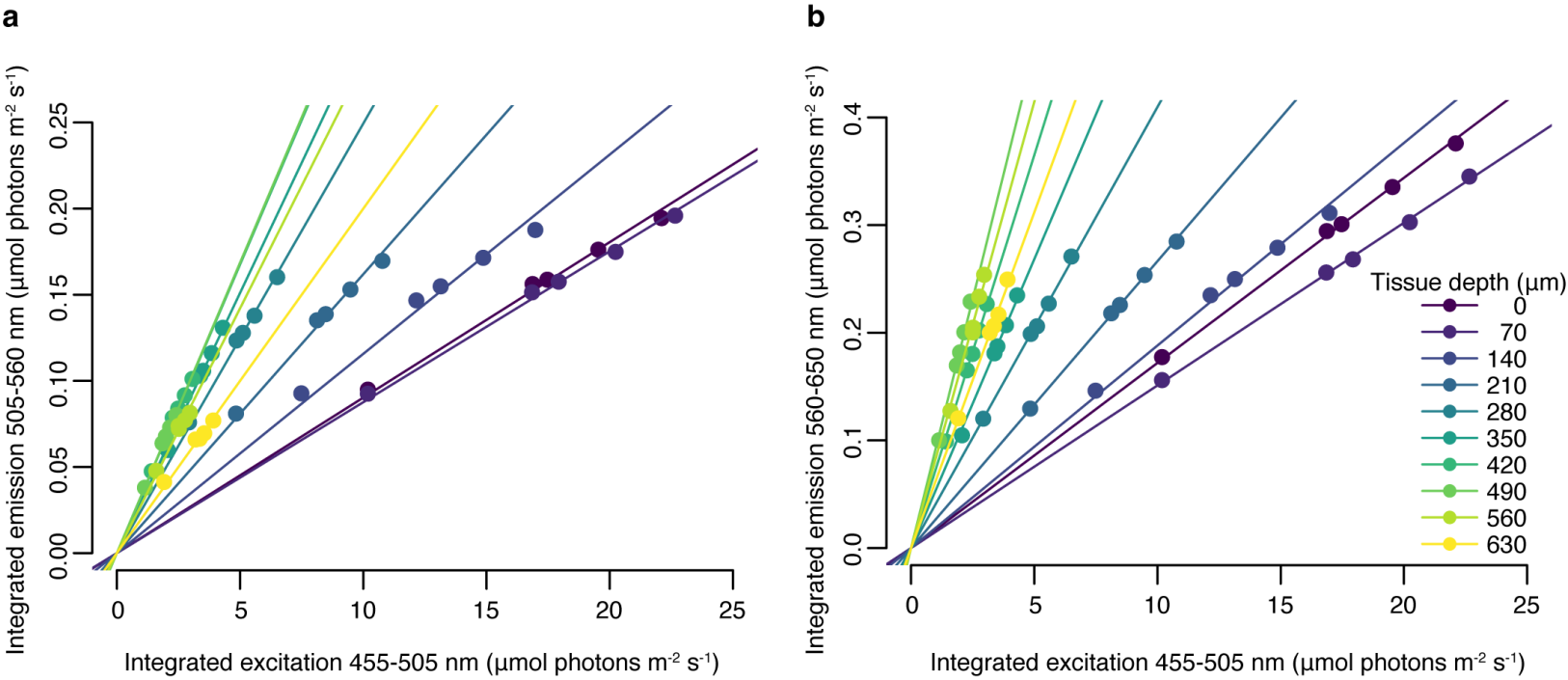
Appendix 1 - figure 1